REGISTERED No. M. 3121

UNIVERSITY OF MICHIGAN
DEC 1 1957
PHYSICS LIBRARY

PROCEEDINGS
OF THE
INDIAN ACADEMY
OF SCIENCES

VOL. XLVI] *SECTION A* [No. 4

OCTOBER 1957

Price Rs. 2 or 3 Sh. *Annual Subscription Rs. 18*

PRINTED AT THE BANGALORE PRESS, BANGALORE CITY, BY C.
SUPERINTENDENT, AND PUBLISHED FOR THE INDIAN ACADEMY OF
SCIENCES, BANGALORE.

EMISSION SPECTRUM OF BROMINE EXCITED IN THE PRESENCE OF ARGON—PART I

By Putcha Venkateswarlu, F.A.Sc. and R. D. Verma

(Department of Physics, Muslim University, Aligarh)

Received May 30, 1957

Abstract

Bromine was excited by an uncondensed transformer discharge in the presence of argon. The spectrum obtained was found to be different from what one gets without the presence of a foreign gas and consists of (1) a short discrete band system in the region 3150–2970 Å, (2) an extensive discrete band system in the region 2950–2670 Å, (3) a short and weak discrete system in the region 2660–2590 Å and a set of diffuse bands in the region 3340–3190 Å. The wavelengths and wave numbers of the band heads of the system 2950–2670 Å, as obtained from the measurements of the plates taken on the first order 21-ft. grating spectrograph, are given along with the vibrational analysis. This system is shown to be due to a transition from an upper electronic state at 51802 cm.$^{-1}$ with $\omega_e' = 150 \cdot 5$ cm.$^{-1}$ and $\omega_e' x_e' = 1 \cdot 15$ cm.$^{-1}$ to the well known $^3\Pi_u$ (O_u^+) state at 15918 cm.$^{-1}$

Introduction

The emission spectrum obtained by electrical excitation of bromine vapour is known to consist of bands degraded to longer wavelength in the region[1,2] 6700–4400 Å and a number of groups of diffuse bands and continua[3–6] in the region 4200–2000 Å. According to Uchida and Ota[1] and also according to Haranath and Rao[2] these bands could be analysed into two systems which arise from two different initial states and involve a common final level which is different from the ground level. The groups of diffuse bands and continua were explained by Venkateswarlu[5] as due to transitions from different stable upper states to various repulsive states dissociating into normal $^2P + {}^2P$ bromine atoms. The electrical and fluorescent excitations of iodine vapour are known to give a discrete band system in emission in the region[6,7] 6700–5000 Å and groups of diffuse bands[8,9] in the region 4800–2400 Å. The discrete band system in emission is known to be completely identical with that in absorption. The groups of diffuse bands were explained by Venkateswarlu[9] as due to transitions from different upper stable states to various lower repulsive states dissociating into $^2P + {}^2P$ normal iodine atoms. It was known by experiments of earlier workers[10–12] that the spectrum obtained by fluorescent excitation of a mixture of iodine and nitrogen is completely different from the fluorescent spectrum of pure iodine vapour.

Elliott[12] obtained four band systems in the regions 4630–4440 Å, 4321–4041 Å, 3450–3040 Å and 2730–2530 Å. Waser and Wieland[13] excited iodine vapour in the presence of argon gas by a high frequency discharge and reported the last three of the systems obtained by Elliott in fluorescence in the presence of nitrogen. Venkateswarlu[14] later excited iodine by transformer discharge and obtained the above three band systems and also a weak system in the region 2785–2750 Å.

Cameron and Elliott[15] excited bromine in the presence of active nitrogen and reported that the continuum at 2900 Å is superposed by a set of diffuse bands with a separation of about 147 cm.$^{-1}$ He, however, did not give the wavelengths or wave numbers of these bands. Because of the above mentioned results obtained by earlier workers in iodine it was expected that new band systems could be well developed if bromine was excited in the presence of argon. This investigation was therefore taken up in this laboratory and the results obtained are given in this paper.

EXPERIMENTAL DETAILS

Bromine vapour was excited in the presence of argon by an uncondensed transformer discharge. The discharge tube was made of pyrex glass and was 50 cm. in length and 0·8 cm. in diameter. It was fitted with a quartz window on one side and a silvered quartz mirror on the other side. Tungston electrodes were used and were found to be quite satisfactory. Band systems obtained were however checked up by using aluminium electrodes also. Argon marked spectrally pure was obtained from Oxygen Acetylene Co. Bromine was prepared by heating cupric bromide. The vapour was dried by allowing it to pass over P_2O_5 tube attached to the system.

It was found that with the increase of the pressure of argon the original spectrum consisting of the discrete band system of bromine in the visible region and the groups of diffuse bands in the region 4200–2000 Å goes down in intensity and new spectrum appears. By adjusting the pressure of argon it was possible to eliminate the original spectrum (except for faint traces at the intense portions) and obtain only the new spectrum. It may be mentioned that the pressures of argon or bromine in the discharge tube were not measured in these experiments, but the relative pressures were adjusted by the visual observation of the colour and the shape of the discharge.

The new spectrum consists of (1) a short discrete band system in the region 3150–2970 Å which is overlapped by the traces of OH bands, (2) an extensive discrete band system 2950 Å–2670 Å, (3) a short and weak discrete band system in the region 2660–2590 Å and (4) a set of diffuse

bands* with intensity maxima at 3211, 3235, 3263, 3292 and 3335 Å. In this paper the analysis of the band system in the region 2950–2670 Å only will be discussed. The discussion of the other systems will be taken up at a later stage when further work is completed.

It was found that the discrete band system 2950–2670 Å could be well developed in intensity and sharpness by adjusting the pressures of the constituent gases such that the discharge was unstationary twisted ribbon-like in shape and pinkish white in colour. It may be mentioned that the band system is usually overlapped by a continuum which extends to shorter wavelengths. This continuum could be well diminished in intensity if the discharge tube is effectively cooled. The origin of this continuum appears to be similar to that of the continua obtained and explained by Uchida[16] in halogens at high temperatures. This means that probably during the discharge a certain amount of molecular bromine is converted into bromine atoms in normal and excited states which on recombination by the two body collision process emit the continuum. However, if the tube is cooled effectively the kinetic energy of the excited and normal atoms is reduced which in turn diminishes the drift velocity and hence makes the two body collision recombination rare.

The spectra were taken in stagnant condition, but when long exposures were needed fresh quantities of bromine and argon were introduced after every four hours or so. The discharge tube was cooled by using a water jacket between the two electrodes, while the electrodes were cooled by an electric fan.

The spectra were first taken with a medium Hilger quartz spectrograph which has a dispersion of 12·5 Å per mm. at 2900 Å and then with a Hilger E_1 Littrow quartz spectrograph which has a corresponding dispersion of about 4·4 Å per mm. The band system was then photographed with an Eagle mounting 21-ft. grating spectrograph in the first and second orders with the dispersion of 2·6 Å per mm. and 1·3 Å per mm. respectively. Fig. 1 shows the spectra obtained in the first order. The plates were measured with a Carl Zeiss Abbe comparator.

The wavelengths and wave numbers of all the bands, as obtained from an average of four measurements of the plates taken on the first order 21-ft. grating spectrograph, are given in Table I along with their visually estimated relative intensities. Though the individual measurements did not differ

* Electrical excitation of bromine vapour without the presence of argon were reported[6] to show in this region certain diffuse bands with their intensity maxima at 3367, 3337, 3269 and 3239 Å. It is to be ascertained by further work whether any of these bands are common with those obtained in the presence of argon.

TABLE I

Wavelengths, wave numbers and relative intensities of the bands in the system 2950–2670 Å.

I	λ_{air}	ν_{vac}	I	λ_{air}	ν_{vac}
1	2952·5	33860	6	2902·0	34449
2	2952·0	33866	4	2900·6	34466
1	2951·6	33870	0	2900·0	34471
0	2948·0	33911	4	2899·4	34480
1	2946·5	33929	4	2898·8	34487
1	2945·4	33941	0	2898·4	34492
2	2944·8	33948	3	2896·8	34511
0	2944·2	33955	4	2895·9	34521
0	2940·7	33996	2	2894·3	34541
1	2940·4	33999	7	2893·7	34548
0	2940·0	34004	0	2893·3	34553
2	2939·6	34008	2	2892·3	34565
3	2939·2	34013	3	2891·9	34569
0	2938·7	34019	2	2891·4	34575
0	2937·3	34035	0	2891·0	34580
0	2933·7	34077	5	2889·9	34593
6	2933·4	34080	4	2888·6	34609
1	2933·1	34084	2	2887·2	34626
5	2932·7	34088	6	2883·2	34674
1	2932·1	34095	7	2881·8	34690
4	2929·3	34128	7	2881·6	34693
5	2928·7	34135	2	2881·2	34698
1	2928·1	34142	0	2880·0	34712
2	2926·7	34158	1	2879·1	34723
9	2924·2	34187	1	2877·5	34742
7	2923·6	34194	0	2875·2	34770
2	2922·9	34203	5	2871·9	34810
5	2920·7	34228	4	2871·0	34821
8	2920·0	34237	3	2870·2	34830
5	2919·3	34245	0	2869·3	34842
0	2918·3	34257	0	2867·4	34865
4	2916·5	34278	4	2866·0	34882
0	2915·4	34291	2	2864·2	34904
10	2914·2	34304	2	2861·7	34934
10	2913·9	34308	4	2860·3	34951
1	2913·5	34313	5	2859·7	34958
0	2912·6	34324	3	2858·9	34968
1	2911·6	34335	0	2858·5	34973
1	2910·8	34345	0	2857·9	34980
0	2909·2	34364	3	2854·8	35018
5	2908·0	34378	0	2853·0	35041
5	2907·3	34386	1	2851·8	35055
3	2905·2	34411	1	2850·1	35076
6	2904·5	34419	2	2849·0	35090
6	2904·0	34425	5	2848·0	35102
4	2903·4	34432	4	2847·6	35107

TABLE I—(*Contd.*)

I	λ_{air}	ν_{vac}	I	λ_{air}	ν_{vac}
3	2846·4	35122	2	2769·3	36100
1	2843·6	35156	1	2768·7	36107
3	2836·5	35244	4	2767·9	36118
5	2835·8	35253	0	2767·2	36127
2	2835·5	35257	2	2766·4	36137
1	2834·7	35267	2	2765·7	36147
1	2824·7	35392	0	2764·2	36166
2	2824·1	35399	2	2762·6	36187
2	2813·5	35532	0	2761·7	36199
3	2813·0	35539	0	2760·1	36220
2	2812·5	35545	3	2759·2	36232
1	2808·3	35598	4	2758·3	36244
0	2803·8	35655	4	2757·1	36259
3	2802·6	35671	0	2756·3	36270
3	2802·0	35678	0	2755·7	36278
3	2801·5	35685	0	2753·4	36308
0	2800·9	35692	0	2751·7	36330
0	2800·0	35704	2	2750·1	36352
1	2799·4	35711	3	2749·6	36358
0	2794·7	35771	0	2746·9	36394
0	2794·0	35780	2	2745·9	36407
1	2793·4	35788	1	2742·5	36452
1	2793·0	35793	0	2740·9	36474
0	2792·4	35801	0	2737·8	36515
0	2791·9	35807	2	2736·1	36538
2	2791·3	35815	2	2735·2	36550
3	2790·7	35823	0	2734·3	36562
2	2790·2	35829	0	2733·5	36572
0	2789·4	35839	0	2732·1	36591
1	2788·1	35856	0	2730·0	36619
1	2786·6	35875	2	2727·5	36693
0	2786·2	35881	0	2721·9	36728
0	2781·4	35943	0	2719·5	36761
2	2780·7	35952	2	2714·3	36831
3	2780·0	35961	1	2706·8	36933*
4	2779·1	35972	1	2695·3	37091*
0	2778·2	35984	0	2683·8	37250*
0	2776·8	36002	0	2673·6	37392*
1	2770·0	36090	0	2666·8	37487*

(*a*) The bands marked * are diffuse and about 50–60 cm.$^{-1}$ in width and are therefore not included in the vibrational analysis. The wavelengths given represent the centres of the diffuse bands. On the short wavelength side of these diffuse bands there is the weak system 2660–2590 Å.

(*b*) The region 2810–2835 Å was found to consist of some traces of the rotational lines of the OH band. If this OH is eleminated one may find a few more bands than those recorded.

(*c*) The weak bands at 34364 cm.$^{-1}$, 35598 cm.$^{-1}$ and 35704 cm.$^{-1}$ can be represented by ($v' = 16$, $v'' = 38$), ($v' = 17$, $v'' = 19$) and ($v' = 18$ and $v'' = 19$) respectively. These are not included in Table II because to represent these bands the vibrational analysis has to be extended and a number of bands are to be repeated for this extension.

by more than 1 cm.$^{-1}$ from the mean value, it is expected that there might be an error of 3 or 4 cm.$^{-1}$ in the determination of the exact position of the band heads as the neighbouring bands in many cases were found to overlap with one another.

VIBRATIONAL ANALYSIS OF THE BAND SYSTEM 2950–2670

The vibrational scheme of the band system is shown in Table II and the intensity distribution in Table III. The Franck-Condon parabola that one gets is exactly of the form that one expects for the transition involving the observed ω_0' and ω_0'' values.

The vibrational analysis shows that all the bands in the system could be well represented as involving a transition from an upper initial state at 51802 cm.$^{-1}$ to the lower state at 15918 cm.$^{-1}$ with the same $\triangle G''(v+\frac{1}{2})$ values as given by Darbyshire[17] and Brown.[18] The lower state is the $^3\Pi_u$ (O_u^+) state which forms the upper state of the visible absorption band system in the region 8672–5110 Å.

The $\triangle G''(v+\frac{1}{2})$ and $\triangle G'(v+\frac{1}{2})$ values as obtained from the analysis are also shown in Table II. The $\triangle G(v+\frac{1}{2})$ values for the $^3\Pi_u$ (O_u^+) level obtained by Darbyshire and Brown from the studies of the visible absorption band system are also included in the table for comparison. Darbyshire from the analysis of the visible absorption band system indicated the existence of the perturbation of the levels $v=3$ and $v=4$ of the $^3\Pi_u(O_u^+)$ state and the analysis of the present system confirms his observation. Because of this perturbation a single formula of the usual type cannot express accurately the positions of all the band heads in the system. But the vibrational constants ω_0'', $\omega_0''x_0''$ and ω_0', $\omega_0'x_0'$ could be determined fairly accurately by the usual procedure from the observed $\triangle G''(v+\frac{1}{2})$ and $\triangle G'(v+\frac{1}{2})$ values. Since the $\triangle G''(v+\frac{1}{2})$ values are practically the same as those obtained by Darbyshire and Brown, it was found that they could be fairly well represented with the vibrational constants $\omega_0'' = 166{\cdot}1$ cm.$^{-1}$ and $\omega_0''x''_0 = 1{\cdot}84$ cm.$^{-1}$ given by Darbyshire.[17] The $\triangle G'(v+\frac{1}{2})$ values could be fairly well represented with the constants $\omega_0' = 149{\cdot}2$ cm.$^{-1}$ and $\omega_0'x_0' = 1{\cdot}15$ cm.$^{-1}$ The $\triangle G'(v+\frac{1}{2})$ values calculated with these constants are included in Table II for comparison.

ISOTOPIC SHIFTS

The three isotopic species of the bromine molecule are $Br^{79}Br^{79}$, $Br^{79}Br^{81}$, and $Br^{81}Br^{81}$ with an abundance ratio of 1 : 2 : 1 and therefore each band corresponding to the more abundant $Br^{79}Br^{81}$ molecule is expected to have one weak band on the low frequency side and one weak band on the high

TABLE II. *The vibrational scheme of the system* 2950–2670 *Å.*

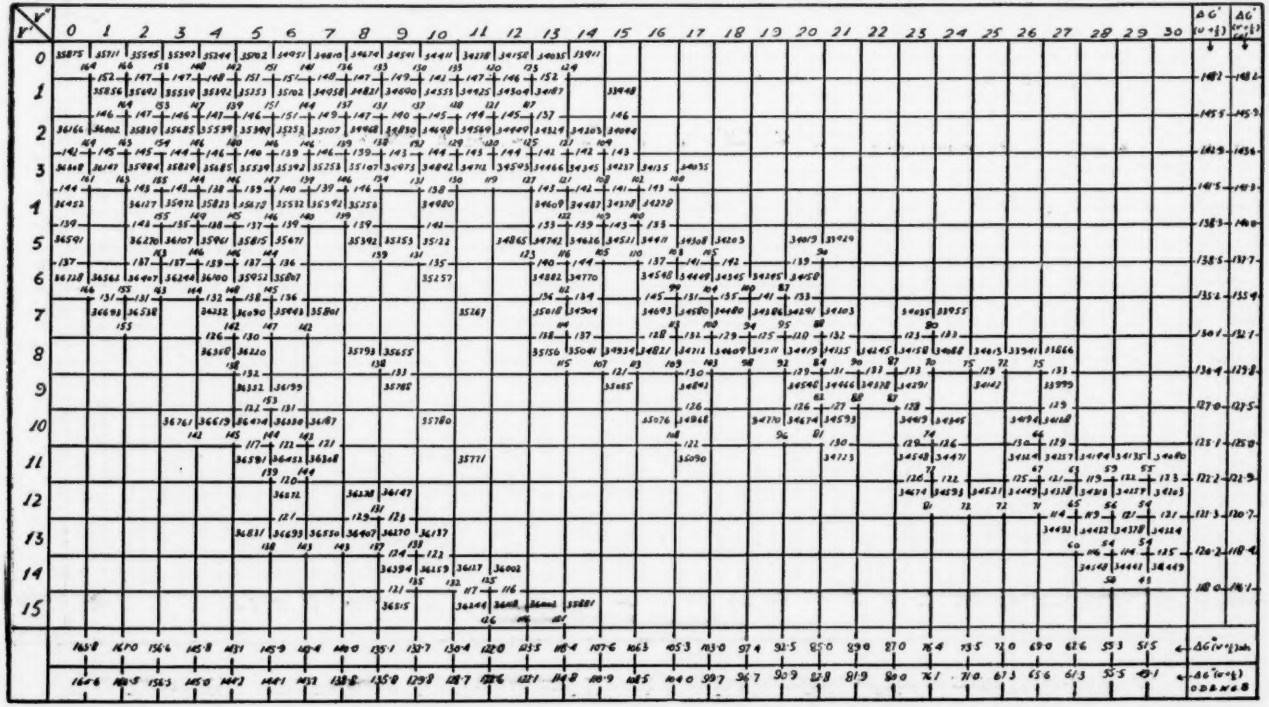

TABLE III. *The intensity distribution and Franck-Condon parabola of the system* 2950–2670 *Å.*

V' \ V''	0	1	2	3	4	5	6	7	8	9	10	11	12	13	14	15	16	17	18	19	20	21	22	23	24	25	26	27	28	29	30
0	1	1	2	1	3	5	4	5	6	2	3	4	2	0	0																
1		1	0	3	1	5	5	5	4	7	0	6	10	9		2															
2	0	0	0	3	3	2	5	4	3	3	2	3	6	0	2	1															
3	0	2	0	2	3	3	1	5	4	0	0	0	5	4	1	8	5	0													
4	1		0	4	3	3	2	1	5		0			4	4	5	4														
5	0		0	1	3	2	3		1	5	3		0	1	2	4	3	10	2		0	1									
6	0	0	2	4	2	2	0				2			4	0		7	6	1	5	2										
7		2	2		3	1	0	0				1		3	2		7	0	4	5	0	2		0	0						
8					3	0			1	0				1	0	2	4	0	4	3	6	1	5	2	5	3	1	2			
9						2	0			1						1		0			7	4	5	0		1		1			
10				0	0	0	0	2			0						1	3		0	6	5		6	1		7	4			
11						0	1	0				0						2				1		7	0		0	0	7	5	6
12							0		0	2														6	5	4	6	5	1	0	2
13						2	2	2	2	0	2																	0	4	5	0
14										0	1	0	0																7	0	6
15										0		1	4	0	0																

frequency side. The vibrational analysis given in Table II corresponds to the molecule $Br^{79}Br^{81}$. The calculated and the probable observed isotopic shifts for some of the strong bands, which could be recognized, are shown in Table IV. For the remaining strong bands the isotopic shifts are either expected to be

TABLE IV

Isotopic shifts of some bands in the system 2950–2670 *Å*

v', v''	ν in cm.$^{-1}$	I	$\Delta\nu_{obs.}$ cm.$^{-1}$	$\Delta\nu_{calc.}$ cm.$^{-1}$
	33860	1		
8, 27	33866	2	5·5	3·8
	33871	1		
	33941	1		
1, 15	33948	2	7·0	9·3
	33955	0		
	33996	0		
9, 27	33999	1	4·0	3·1
	34004	0		
	34008	2		
8, 25	34013	3	5·5	4.6
	34019	0		
	34084	1		
8, 24	34088	5	5·5	4·7
	34095	1		
	34128	5		
3, 16	34135	6	7·0	9
	34142	0		
1, 13	34187	9	7·0	8·5
	34194	7		
	34228	5		
3, 15	34237	8	8·5	7·6
	34245	5		
4, 16	34278	4	6·0	7·1
	34284	0		
1, 12	34304	10	9·0	8·1
	34313	1		

TABLE IV—(*Contd.*)

v', v''	ν in cm.$^{1-}$	I	$\Delta_{obs.}$ cm.$^{-1}$	$\Delta\nu_{calc.}$ cm.$^{-1}$
	34304	10		
5, 17	34308	10	4·5	6·4
	34313	1		
4, 15	34378	5	8·0	6·8
	34386	5		
0, 10	34411	3	8·0	8·5
	34419	6		
	34419	6		
1, 11	34425	6	6·5	7·6
	34432	3		
	34480	4		
4, 14	34487	4	6·0	6·5
	34492	0		
	34541	2		
6, 16	34548	7	6·0	5·5
	34553	0		
	34565	0		
2, 11	34569	3	5·0	6·7
	34575	0		
	34690	7		
7, 16	34693	7	4·0	4·8
	34698	2		
	34951	3		
1, 7	34958	3	8·5	5·2
	34968	3		
0, 6	34951	3	7·0	5·8
	34958	3		
2, 8	34968	3	5·0	5·0
	34973	0		
0, 5	35102	5	5·0	4·9
	35107	4		
2, 6	35253	5	4·0	3·5
	35257	2		

less than 2 cm.$^{-1}$ or are probably overlapped by the neighbouring bands and, therefore, could not be measured.† It is to be noted that a number of the bands which could be represented as belonging to $Br^{79}Br^{79}$ or $Br^{81}Br^{81}$, could also be represented as belonging to $Br^{79}Br^{81}$ with different v', v'' values and therefore also included as such in Table II. This may be the reason why the expected ratio of the relative intensities among the three bands belonging to three isotopic species is not maintained. For some of the bands, isotopic shifts on the short wavelength side only could be observed. The one on the long wavelength side is probably masked by the main band ($Br^{79}Br^{81}$) which is degraded to longer wavelengths. Agreement between the calculated and the probable observed isotopic shifts supports the correctness of the vibrational analysis given.

The Electronic Transition Involved

As stated earlier, the lower state of the system is the $^3\Pi_u$ (O_u^+) level with the configuration $\sigma_g{}^2\pi_u{}^4\pi_g{}^3\sigma_u$. As regards the upper state it is difficult to say definitely which electronic state is involved, unless the rotational structure of the bands is studied. The second order plates and a fourth order plate tried for the strong portion of the spectrum could only show partially resolved structure. It is expected that it would probably be easy to obtain the rotational structure of the analogous system‡ in chlorine and decide about the upper electronic term involved.

However, with the help of the term scheme developed by Mulliken[20] for iodine molecule and later extended by Asundi and Venkateswarlu[6] to bromine molecule one can see that the only configuration that is expected to give "*gerade*" states around 50,000 cm.$^{-1}$ is $\sigma_g{}^2\pi_u{}^2\pi_g{}^4\sigma_u{}^2$. This configuration gives the states $^1\Sigma_g^+$ (O_g^+), $^3\Sigma_g^-$ (O_g^+, 1_g) and $^1\triangle_g$ (2_g), of which the last cannot combine with the $^3\Pi_u$ (O_u^+) state as the coupling is expected

† It is probably because of similar reasons that only few isotopic displacements were measured by earlier workers,[18, 17] in the absorption band systems of bromine in the visible and near infrared regions. Brown [18] recorded isotopic shifts for only 18 bands out of a total number of 90 bands put by him in the Deslandres scheme for the visible absorption band system (6950–5110 Å). Darbyshire[17] extended the system upto 8672 Å and arranged 22 new bands in the extension of the Deslandres scheme, but could measure only twelve possible isotopic displacements of which he was sure six to be free from overlapping of other bands. Similarly in the system 6450–8150 Å he could measure only three isotopic displacements.

‡ Cameron and Elliott[15] excited chlorine in presence of active nitrogen and obtained a set of closely spaced bands in the region 2580–2380 Å where only two continua show up with the intensity maxima at 2565 Å and 2430 Å, if chlorine is excited electrically[21, 22] without the presence of a foreign gas. They gave the wavelengths of these bands as obtained with a medium quartz spectrograph. The wave number separation of the bands in the progressions suggests that the band system probably involves the $^3\Pi_u$ (O_u^+) state and therefore, is analogous to the present band system of bormine. Further work on this chlorine system is in progress in this laboratory.

to be nearer to that of Hund's case (*c*). The calculated average position of the states that arise from $\sigma_g^2\pi_u^2\pi_g^4\sigma_u^2$ is 6·0 ev. and $^1\Sigma_g^+(O_g^+)$ is expected to be higher than $^3\Sigma_g^-(O_g^+, 1_g)$. The position of the upper state of the present band system is at 51802 cm.$^{-1}$ or 6·4 ev. and one can therefore tentatively assign $^1\Sigma_g^+(O_g^+)$ to this state. The presence of the two strongly antibonding electrons explains the low value of the vibrational frequency of the state which is less than half of the ground state. The probable ionic character predicted by Mulliken[20] for this state suggests a high value for the dissociation energy§ of this state.

THE EFFECT OF THE FOREIGN GAS

When bromine is excited without the presence of argon gas, the region 2980–2680 Å shows two groups of diffuse bands. The first group consists of six diffuse bands with the most intense one at 2900 Å, while the second group consists of five diffuse bands with the most intense one at 2754 Å. Unless the spectrum is taken on plates showing good contrast, these groups of diffuse bands appear as two continua with maxima at 2900 Å and 2754 Å respectively. The average separation of the constituent bands in both the groups is of the order of 330 cm.$^{-1}$ Venkateswarlu[5] explained these two groups of bands along with others as arising in an upper stable *gerade* electronic state at about 55534 cm.$^{-1}$ and having for the final levels two unstable *ungerade* states dissociating into $^2P_{3/2}+ {}^2P_{1/2}$ bromine atoms. The mutual separation of the diffuse bands gave the frequency of the upper state. It appears that when bromine is excited electrically, the electronic state at 55534 cm.$^{-1}$ which has the same r_e value as the ground state, is very easily reached and groups of intense diffuse bands occur because of transitions to

§ It may be pointed out that the linear extrapolation method using the values $\omega_0' = 149{\cdot}35$ cm.$^{-1}$ and $\omega_0'x_0' = 1{\cdot}15$ cm.$^{-1}$ gives $D_e = 4849$ cm.$^{-1}$ and $D_e = 4924$ cm.$^{-1}$ for the dissociation energy of the state which will then have the dissociation limit at 56726 cm.$^{-1}$ This value can be seen to be much lower than the levels of the lowest possible dissociation products. This anomaly can be understood if one considers this state to be an ionic state and remembers as pointed out by Gaydon[23] that the linear extrapolation method cannot be used to obtain the dissociation energy of the ionic state as it was found in many cases to give values very much lower than the correct ones. It is to be noted further that the $\Delta G'(v+\frac{1}{2})$ values are observed only upto $v' = 15$ and it is too much to attempt to find the dissociation energy of this state with these few $\Delta G'(v+\frac{1}{2})$ values. However, it can be pointed out that the last two observed $\Delta G'(v+\frac{1}{2})$ values indicate the existence of a positive cubic term $(\omega_0 y_0 v^3)$ which will, of course, take up the dissociation limit to higher values. It will always be possible to adjust the higher order terms in such a way that the calculated values agree well with the few observed $\Delta G'(v+\frac{1}{2})$ values and at the same time give as much high dissociation energy as we want. For instance the vibrational constants $\omega_0' = 149{\cdot}35$ cm.$^{-1}$, $\omega_0'x_0' = 1{\cdot}25$ cm.$^{-1}$, $\omega_0'y_0' = 0{\cdot}01$ cm.$^{-1}$ and $\omega_0'z_0' = 0{\cdot}00003$ cm.$^{-1}$ give $\Delta G'(v+\frac{1}{2})$ values in agreement with those observed and give a dissociation energy of about 14,000 cm.$^{-1}$

different repulsive states. When the foreign gas is introduced, collisions take place and the molecule is taken away from the stable state at 55534 cm.$^{-1}$ to the different vibrational levels of the stable state at 51802 cm.$^{-1}$ having smaller ω_e value and therefore larger r_e value. Transition then takes place from this state to the $^3\Pi_u(O_u^+)$ state at 15918 cm.$^{-1}$ which has also a large r_e value. As one increases the pressure of the argon gas, more molecules reach the state at 51802 cm.$^{-1}$ by collisions and the discrete band system 2950–2670 Å increases in intensity while the group of diffuse bands in the region decrease in intensity.

Further Remarks

At 940° C. and 270 mm. pressure of bromine Dabrowski[24] obtained in absorption a weak band near 2930 Å with a sharp limit on the long wavelength side. This absorption may probably correspond to the first group of the overlapping diffuse bands mentioned above in emission. The occurrence of this absorption at high temperature can be explained as a transition from the repulsive state reached by the recombination of the $^2P_{3/2}+\ ^2P_{1/2}$ bromine atoms to the upper stable state at 55534 cm.$^{-1}$, the bromine atoms having been probably obtained by thermal dissociation of molecules at high temperature. This view is supported by the fact that at high temperatures Uchida[16] obtained in thermal luminescence a discrete band system in the visible region which is completely identical with the visible absorption band system and which can be explained only on the basis that the initial state $^3\Pi_u(O_u^+)$ of the system is formed by the recombination of $^2P_{3/2}+\ ^2P_{1/2}$ bromine atoms.

This absorption along with that of Dabrowski incidentally suggests that the band system 2950–2670 Å discussed in the present paper may be observed in absorption at high temperatures if proper conditions of temperature and pressure are reached. The intensity of this system in absorption will, of course, depend upon the life-time of the molecules in the $^3\Pi_u(O_u^+)$ state.

Acknowledgement

The authors wish to express their thanks to Prof. R. K. Asundi for permission to use the 21-ft. grating spectrograph at Banaras Hindu University and for the hospitality shown to one of them (R. D. Verma) while working at Banaras. They are also thankful to the U.P. Research Grant Committee for financial assistance and to Prof. P. S. Gill for his kind interest in the development of this work.

REFERENCES

1. Uchida, Y. and Ota, Y. .. *Jap. Jour. Phys.* (*Tokyo*), 1928, **5**, 59.
2. Haranath, P. B. V. and Rao, P. T. *Ind. Jour. Phys.*, 1955, **29**, 205.
3. Strutt, R. J. and Fowler, A. .. *Proc. Roy. Soc.* (*London*), 1912, **86 A**, 105.
4. Ludlam, B. and West, W. .. *Ibid.*, *Edinburgh*, 1923–24, **44**, 85.
5. Venkateswarlu, P. .. *Proc. Ind. Acad. Sci.*, 1947, **25**, 138.
6. Asundi, R. K. and Venkateswarlu, P. *Ind. Jour. Phys.*, 1947, **21**, 101.
7. Herzberg, G. .. *Spectra of Diatomic Molecules*, D. Van Nostrand Company, New York, 1950.
8. Asagoe, K. and Inuzuka, Y. .. *Sci. Rep. Tokyo Burnika Daigaku*, 1934, **2 A**, 73.
9. Venkateswarlu, P. .. *Proc. Ind. Acad. Sci.*, 1946, **24 A**, 480; *Ibid.*, 1947, **25 A**, 119 and 133. (Earlier references on Iodine are given in these papers.)
10. Oldenburg, O. .. *Z. Physik.*, 1924, **25**, 135.
11. Duchinsky, F. and Pringsheim, P. *Physica*, 1935, **2**, 923.
12. Elliott, A. .. *Proc. Roy. Soc.* (*London*), 1940, **174 A**, 273.
13. Waser, J. and Wieland, K. .. *Nature*, 1947, **160**, 643.
14. Venkateswarlu, P. .. *Phys. Rev.*, 1951, **81**, 821.
15. Cameron, W. H. B. and Elliott, A. *Proc. Roy. Soc.* (*London*), 1938–39, **169 A**, 463. (*See* Footnote on p. 465 of this article.)
16. Uchida, Y. .. *Sci. Papers Inst. Phys. Chem. Res.*, 1936, **30**, 71.
17. Darbyshire, O. .. *Proc. Roy. Soc.* (*London*), 1937, **159**, 93.
18. Brown, W. G. .. *Phys. Rev.*, 1931, **38**, 1179–86.
19. ——— .. *Ibid.*, 1932, **39**, 777–87.
20. Mullikan, R. S. .. *Ibid.*, 1934, **46**, 549.
21. Elliott, A. and Cameron, W. H. B. *Proc. Roy. Soc.* (*London*), 1937, **158 A**, 681.
22. Venkateswarlu, P. .. *Proc. Ind. Acad. Sci.*, 1947, **26 A**, 22.
23. Gaydon, A. G. .. *Dissociation Energies and Spectra of Diatomic Molecules*, Chapman and Hall Ltd., London, 1947.
24. Dabrowski, L. .. *Acta Physica Polonica*, 1934, **3**, 301.

EXPLANATION OF PLATES

PLATES X AND XI

FIG. 1. (*a*), (*b*) & (*c*) Enlargements of the band system 2950–2670 A of bromine photographed in the 1st order of 21 ft. grating spectrograph.

(*d*) Extra enlargement of the band system 2950–2670 A in the region 2940–2830 A showing bipbaroe isotopic shifts.

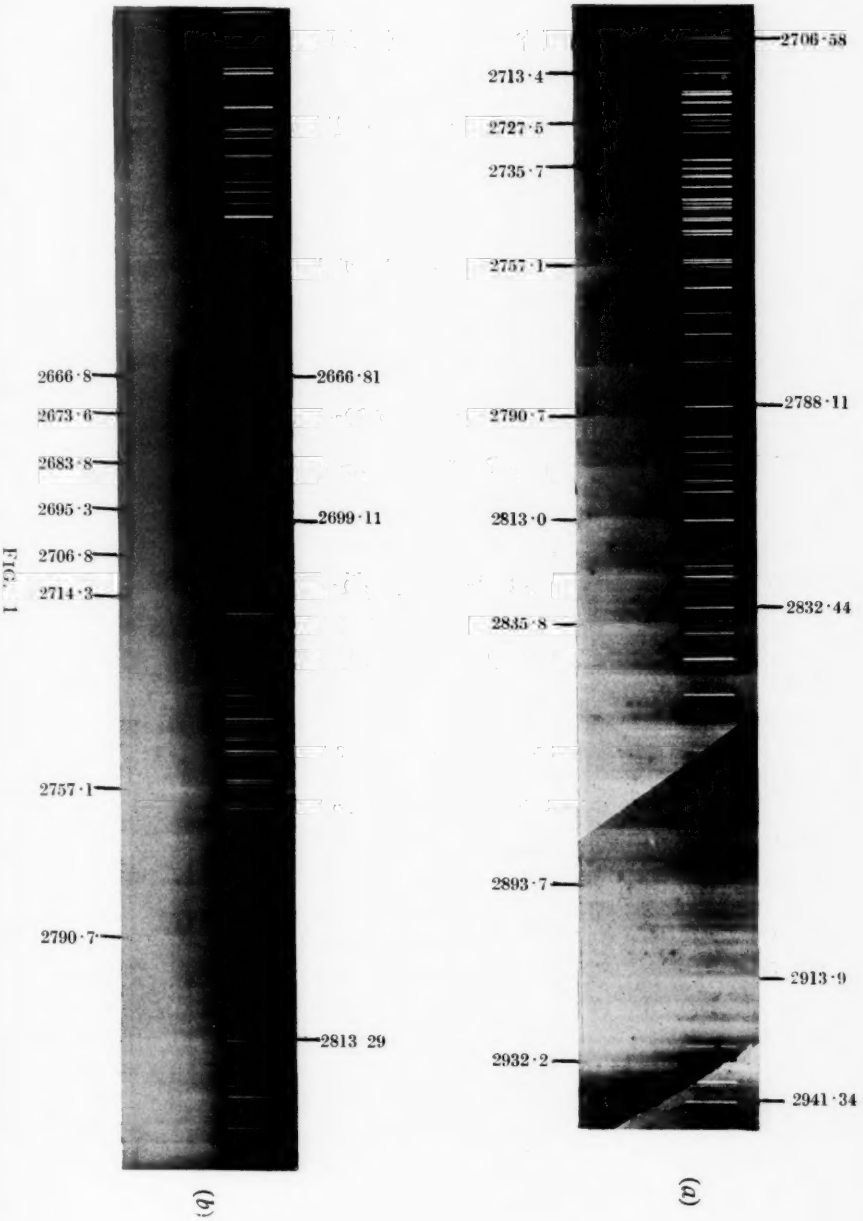
2666·8
2673·6
2683·8
2695·3
2706·8
2714·3
2757·1
2790·7
2666·81
2699·11
2813 29
2706·58
2713·4
2727·5
2735·7
2757·1
2790·7
2813·0
2835·8
2893·7
2788·11
2832·44
2913·9
2932·2
2941·34
(a)
(b)

FIG. 1

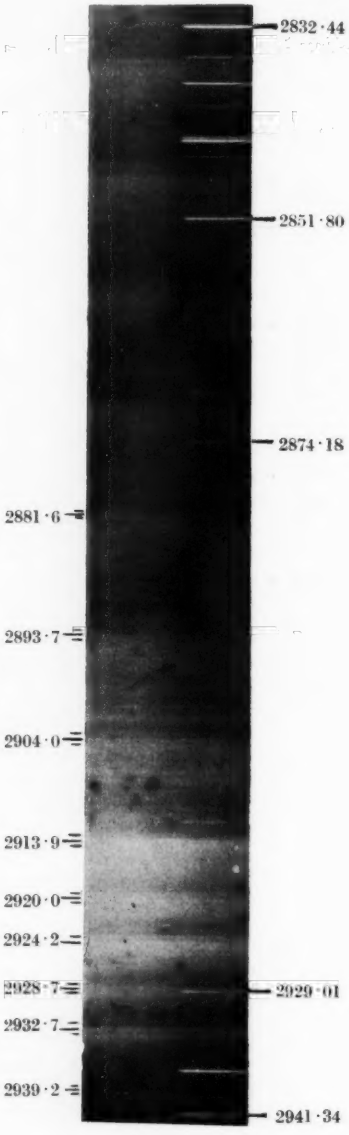
2832·44
2851·80
2874·18
2881·6
2893·7
2904·0
2913·9
2920·0
2924·2
2928·7
2932·7
2939·2
2929·01
2941·34

(*d*)

2699·11
2714·3
2727·5
2735·2
2745·9
2757·1
2767·9
2779·1
2790·7
2802·0
2848·0
2893·7
2788·11
2813·29
2851·80
2874·18
2913·9
2928·1
2947·18

(*c*)

FIG. 1

SYNTHETIC EXPERIMENTS IN THE BENZOPYRONE SERIES

Part LXVI. Relative Stability of Isomeric 6-Methyl and 8-Methyl-Trihydroxy Flavones

By V. V. S. Murti, T. R. Seshadri, F.A.Sc., V. Sundaresan and B. Venkataramani

(Department of Chemistry, Delhi University, Delhi)

Received August 22, 1957

In a recent publication[1] Mukerjee, Rajagopalan and Seshadri reported the preparation of 2:8-dimethyl-5:6:7-trihydroxy (I *a*) and 2:6-dimethyl-5:7:8-trihydroxy (II *a*) chromones and their derivatives. They subjected their methyl ethers to demethylation with hydriodic acid; the methyl ether of (I *a*) underwent only demethylation and no isomeric change whereas the methyl ether of (II *a*) underwent demethylation and complete isomerisation. This showed that for maximum stability the 6-position for the hydroxyl and the 8-position for methyl are the most favourable. In order to test the validity of the conclusion to other groups of compounds a similar study has now been made using analogous flavone derivatives, *i.e.*, 5:6:7-trihydroxy-8-methyl flavone (I *b*) and 5:7:8-trihydroxy-6-methyl flavone (II *b*).

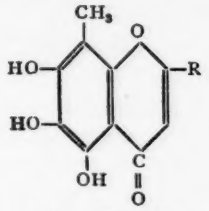

I *a*, R = CH_3
b, R = C_6H_5

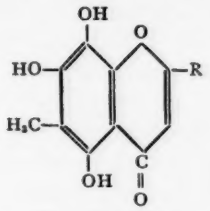

II *a*, R = CH_3
b, R = C_6H_5

The most convenient method for the preparation of flavone (I *b*) is to start with 8-methyl chrysin (III) whose preparation has already been described.[2] It is converted into the corresponding 6-aldehyde (IV) by the hexamine method and subsequent Dakin oxidation in tetramethyl ammonium hydroxide solution[3] yields 8-methyl baicalein (I *b*). Methylation under appropriate conditions gives its 6 : 7: di- and 5:6:7-trimethyl ethers. These suffer demethylation with hydriodic acid under ordinary conditions giving solely 8-methyl baicalein and there is no isomeric change.

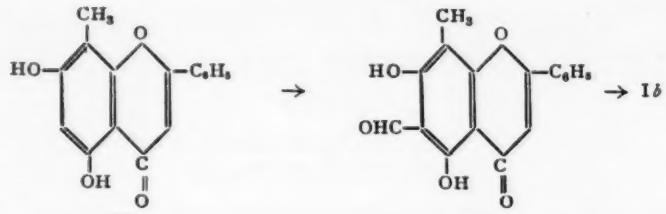

8-Methyl baicalein can also be prepared by an alternative method starting from 2-hydroxy-3-methyl-4 : 6-dimethoxy acetophenone[4] (V *a*); the steps are indicated in the following formulæ. It may be mentioned in this connection that this is the first instance of the successful application of Baker-Venkataraman isomerisation (Wheeler modification[5]) to a quinol derivative.

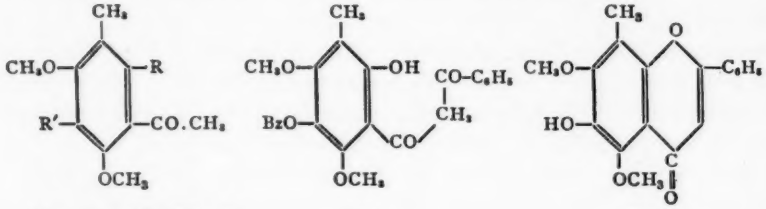

V *a*, R = OH, R′ = H
b, R = R′ = OH
c, R = R′ = O·Bz

VI

VII

For the preparation of the isomeric 6-methyl-5 : 7 : 8-trihydroxy flavone (II *b*), norwogonin (VIII) was subjected to nuclear methylation whereby 5-hydroxy-7 : 8-dimethoxy-6-methyl flavone (IX) was obtained along with a larger amount of 5-hydroxy-7 : 8-dimethoxy flavone; the two could be separated by chromatography over alumina or ' magnesol '. When subjected to demethylation with hydriodic acid, (IX) suffers demethylation and complete isomeric change into 8-methyl baicalein (I *b*). Thus the flavone derivatives behave very similar to the corresponding chromones. However, for the preparation of 6-methyl norwogonin (II *b*) demethylation of the dimethyl ether (IX) with aluminium chloride in benzene solution was found to be suitable. Attempts to prepare this compound by the nuclear oxidation of 6-methyl chrysin with alkaline persulphate were unsuccessful.

EXPERIMENTAL

5 : 7-*Dihydroxy*-8-*methyl flavone*-6-*aldehyde* (*IV*).—5 : 7-Dihydroxy-8-methyl flavone (III) required for this work was prepared according to the procedure of Mukerjee and Seshadri[2]; in the isomerisation of 2-benzoyloxy-3-methyl-4 : 6-dimethoxy acetophenone to the diketone, the pyridine-potash

method of Wheeler was found to be more convenient and gave better yields than the sodamide-toluene method.

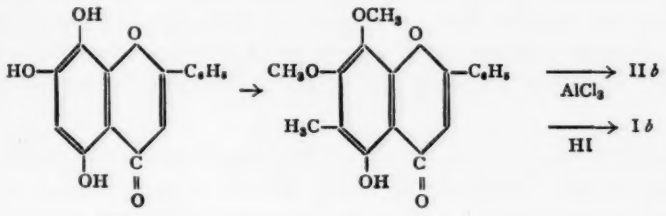

VIII IX

A mixture of 8-methyl chrysin (1·2 g.) in glacial acetic acid (100 c.c.) and hexamine (4 g.) was heated in a boiling water-bath for 6 hours. The deep red solution was treated with concentrated hydrochloric acid (20 c.c.) and the heating continued for another 20 minutes when a pale yellow solid separated. The mixture was diluted with a large volume of water and left overnight in the refrigerator. The aldehyde crystallised from benzene or glacial acetic acid as pale yellow, soft, flat needles (0·7 g.), m.p. 255–56°; mixed m.p. with 8-methyl chrysin, 220° (Found: C, 68·7; H, 4·2; $C_{17}H_{12}O_5$ requires C, 68·9 and H, 4·1%). The aldehyde is sparingly soluble in alcohol, acetone and ethyl acetate but more soluble in hot benzene and hot glacial acetic acid. It is not readily soluble in aqueous sodium hydroxide and on warming formed a yellow, sparingly soluble sodium salt. It gave a red-brown ferric reaction. The *dinitrophenyl hydrazone* of the aldehyde formed orange-red tiny needles, m.p. 330° (decomp.).

The aldehyde gave the *tetra-acetate* on acetylation in the cold with acetic anhydride and a drop of concentrated sulphuric acid; colourless plates (from acetone), m.p. 236–37° (gas evolution) (Found: C, 62·6; H, 4·9; $C_{25}H_{22}O_{10}$ requires C, 62·2 and H, 4·6%).

5:6:7-*Trihydroxy*-8-*methyl flavone* (*I* b).—The foregoing aldehyde (1·0 g.) was suspended in pyridine (30 c.c.) and tetramethyl ammonium hydroxide (10%; 10 c.c.) added. The red solution was cooled in ice-water, nitrogen bubbled through it for 10 minutes and hydrogen peroxide (6%; 3 c.c.) was added dropwise with vigorous shaking; the solution turned dark brown. Nitrogen was passed for another 2 hours, the reddish-yellow solution heated to 50° and acidified with dilute sulphuric acid. The yellow solid crystallised from methanol as tiny yellow prisms (0·5 g.) turning brown at 220° and melting at 286–88° (decomp.) (Found: C, 67·3; H, 4·4; $C_{16}H_{12}O_5$ requires C, 67·6 and H, 4·2%).

The compound gives a brown-black ferric reaction which turns brown on standing. With aqueous sodium hydroxide a bluish-green solution is obtained which turns green on shaking; on standing a dark green precipitate settles and the solution becomes colourless. Treatment with sodium amalgam in alcoholic solution yields a deep green solution from which a green precipitate separates gradually the solution becoming yellow (Bargellini's test).

The *triacetate* prepared by the acetic anhydride-sulphuric acid method crystallised from alcohol as colourless prisms, m.p. 214–15°.

5-*Hydroxy*-6: 7-*dimethoxy*-8-*methyl flavone*.—8-Methyl baicalein (0·4 g.) was partially methylated by refluxing with dimethyl sulphate (0·3 c.c.) and potassium carbonate (5 g.) in dry acetone (50 c.c.) for 6 hours. The dimethyl ether crystallised from isopropyl alcohol (charcoal) as yellow, thin plates, m.p. 159–60°. It gave a deep green ferric reaction (Found: C, 69·7; H, 5·5; $C_{18}H_{16}O_5$ requires C, 69·2 and H, 5·1%).

5: 6: 7-*Trimethoxy*-8-*methyl flavone*.—8-Methyl baicalein (0·6 g.) was completely methylated by refluxing with dimethyl sulphate (2 c.c.) and potassium carbonate (8 g.) in dry acetone (200 c.c.) for 32 hours. The methyl ether was purified by chromatography over alumina and elution with benzene. It crystallised from dilute methanol as colourless, small plates, m.p. 133–34° (Found: C, 69·6; H, 5·8; $C_{19}H_{18}O_5$ requires C, 69·9 and H, 5·5%).

2: 5-*Dihydroxy*-3-*methyl*-4: 6-*dimethoxy acetophenone* (*V* b).—Oxidation of 3-methyl phloracetophenone dimethyl ether[3] (2·1 g.) was carried out in a cold mixture of pyridine (50 c.c.) and aqueous potassium hydroxide (2·8 g. in 40 c.c. water) by the dropwise addition (mechanical stirring) of a solution of potassium persulphate (3·5 g. in 150 c.c. water). The quinol isolated as usual crystallised from benzene-petroleum ether as yellow small prisms (0·6 g.), m.p. 119–20° (Found: C, 58·5; H, 6·4; $C_{11}H_{14}O_5$ requires C, 58·4 and H, 6·2%).

The quinol gave a transient green colour with alcoholic ferric chloride; the solution turned deep red with more of the reagent. It dissolved readily in aqueous sodium hydroxide to give a bright yellow solution; on shaking with air the colour faded, then became pale pink which gradually disappeared.

2: 5 - *Dibenzoyloxy* - 3 - *methyl* - 4: 6-*dimethoxy-acetophenone* (*V* c).—The above quinol (2 g.) was heated with benzoyl chloride (4 c.c.) and dry pyridine (15 c.c.) for 2 hours on a boiling water-bath. Ice-water was added and after standing overnight the mixture was extracted with ethyl acetate, the extract

was washed with dilute soda, dilute acid and water. Removal of the solvent left a viscous oil which quickly solidified. The dibenzoate crystallised from alcohol as colourless, thick prisms, m.p. 175–76° (Found: C, 68·6; H, 5·4; $C_{25}H_{22}O_7$ requires C, 69·1 and H, 5·1%).

Isomerisation of the dibenzoate to the diketone (*VI*).—The dibenzoate (1·5 g.) was dissolved in warm, dry pyridine (20 c.c.) and vigorously shaken with powdered potassium hydroxide (1 g.) with occasional warming on a water-bath. The mixture turned yellow and after 15 minutes a yellow salt separated. After shaking for one hour, acetic acid was added and then diluted with a large volume of water. The sticky material solidified on cooling and scratching and crystallised from ethanol as yellow, irregular prisms (0·7 g.), m.p. 135-36°. It gave a greenish-brown ferric reaction (Found: C, 69·7; H, 5·2; $C_{25}H_{22}O_7$ requires C, 69·1 and H, 5·1%).

6-*Hydroxy*-5: 7-*dimethoxy*-8-*methyl flavone* (*VII*).—Ring closure of the diketone to the flavone was effected by heating with fused sodium acetate in glacial acetic acid solution for 2 hours. The colourless solid obtained on dilution was dissolved in warm alkali and the alkaline solution acidified. The flavone crystallised from methyl alcohol as almost colourless small prisms, m.p. 227–28°. It did not give any colour with alcoholic ferric chloride (Found: C, 69·5; H, 5·5; $C_{18}H_{16}O_5$ requires C, 69·2 and H, 5·1%).

Methylation of the hydroxy compound by the methyl sulphate-potassium carbonate-acetone method yielded 8-*methyl*-5: 6: 7-*trimethoxy flavone* identical with the sample already described.

Action of hydriodic acid on 8-*methyl baicalein and its methyl ethers.*—A mixture of 8-methyl baicalein (0·8 g.), acetic anhydride (15 c.c.) and hydriodic acid (15 c.c., *d.* 1·7) was refluxed for 3 hours and then diluted with saturated sodium bisulphite solution. The yellow solid on crystallisation from alcohol melted at 286–88° (decomp.) and did not depress the m.p. of an authentic specimen of 8-methyl baicalein. Similar treatment of 8-methyl baicalein 6: 7-di- and 5: 6: 7-trimethyl ethers also yielded 8-methyl baicalein identified by m.p., mixed m.p. and colour reactions.

Nuclear methylation of norwogonin (*VIII*) *to* 5-*hydroxy*-7: 8-*dimethoxy*-6-*methyl flavone* (*IX*).—Norwogonin required for this experiment was prepared by the method of Sastri and Seshadri.[6] The only modification introduced was that the 2-benzoyloxy-3: 4: 6-trimethoxy acetophenone was converted into the diketone by the pyridine-potash method of Wheeler[5] which was convenient and the yields were good.

Norwogonin (1·0 g.) was dissolved in ice-cold absolute methanol (75 c.c.) containing sodium methoxide from 1·4 g. of sodium. The deep blue-green solution was treated with methyl iodide (10 c.c.) and the mixture was gently shaken for an hour. It was then refluxed for 4 hours on a water-bath during which period the colour of the solution became brown. Methanol was removed under reduced pressure, dilute hydrochloric acid added and the brown solid was filtered. It was extracted with hot benzene, and the benzene solution passed through 'magnesol' which was eluted with more benzene (100 c.c.). The benzene eluate on evaporation left a yellow residue which crystallised from ethyl alcohol as yellow, long needles (50 mg.), m.p. 256–57° (Found: C, 69·3; H, 5·1; $C_{18}H_{16}O_5$ requires C, 69·2 and H, 5·1%). It gave a green ferric chloride colour.

Further elution with benzene-acetone (1 : 1) gave 5-hydroxy-7 : 8-dimethoxy flavone (0·3 g.), m.p. 176–77°.

Action of hydriodic acid on (*IX*).—5-Hydroxy-7 : 8-dimethoxy-6-methyl flavone (IX) (0·1 g.) was refluxed with acetic anhydride (2 c.c.) and hydriodic acid (2 c.c.; *d*. 1·7) for 3 hours. The product on crystallisation from methanol melted at 286–88° and did not depress the m.p. of an authentic sample of 8-methyl baicalein. It also showed the same colour reactions as the latter.

5 : 7 : 8-*Trihydroxy*-6-*methyl flavone* (*II* b).—5-Hydroxy-7 : 8-dimethoxy-6-methyl flavone (0·1 g.) was refluxed with aluminium chloride (0·3 g.) in dry benzene (5 c.c.) solution for 2 hours. On working up as usual 6-methyl norwogonin crystallised from alcohol as deep yellow long needles turning brown at 240° and melting at 265–67° (decomp.). It gave a greenish-brown ferric chloride colour which changed to brown on standing. On reduction with sodium amalgam in alcoholic solution a transient orange brown colour was produced and the solution quickly became colourless (Found: C, 67·2; H, 4·2; $C_{16}H_{12}O_5$ requires C, 67·6 and H, 4·2%).

SUMMARY

8-Methyl baicalein has been made (1) from 8-methyl chrysin by the preparation of the 6-aldehyde and subsequent Dakin's reaction and (2) from C-methyl phloracetophenone dimethyl ether by steps involving persulphate oxidation and flavone ring closure. The isomeric 6-methyl compound has been obtained by the nuclear methylation of norwogonin and demethylation with aluminium chloride. The methyl ethers of the former undergo only demethylation when boiled with hydriodic acid whereas those of the latter undergo isomeric change besides demethylation.

References

1. Mukerjee, Rajagopalan and Seshadri — *J. Sci. Ind. Res.*, 1957, **16 B,** 58.
2. —— and Seshadri .. *Proc. Ind. Acad. Sci.*, 1953, **38 A,** 207.
3. Baker *et al.* .. *J.C.S.*, 1953, 1615.
4. Curd and Robertson .. *Ibid.*, 1933, 437.
5. Doyle *et al.* .. *Proc. Roy. Dublin Soc.*, 1948, **24,** 291.
6. Sastri and Seshadri .. *Proc. Ind. Acad. Sci.*, 1946, **24 A,** 243.

THE LOCALISATION OF THE DISCHARGE CHANNEL IN A GLOW DISCHARGE

By Dr. V. T. Chiplonkar, J. Mangaly and Kumari D. V. Nagamani
(*Physics Department, Institute of Science, Bombay*)

Received May 31, 1957
(Communicated by Dr. R. K. Asundi, F.A.SC.)

Abstract

The localisation of the discharge channel under the conditions of a glow discharge in air, at different distances from the cathode and at various points in the cathode dark space for different voltages, has been studied by measuring the radial distribution of the light intensity in the discharge channel. It has been shown that the radial ion distribution which has a flat maximum at lower voltages changes over into an approximately Gaussian one as the discharge voltage is increased. In the former case the width of the flat maximum decreases as the ion-channel proceeds towards the cathode. At higher voltages ($\sim$ 6 kV.) the flat maximum type of distribution in the ion-channel progressively changes over into the Gaussian as the channel approaches the cathode.

The localisation[1–4] of the discharge channel under the conditions of a glow discharge has been extensively studied experimentally because of its importance both from the point of view of the mechanism of the discharge and of the efficiency of the tube as a canal ray source of ions. It is only recently that Kamke[4] has offered a theory of the effect in terms of the following processes occurring in the dark space under the conditions of an abnormal discharge. (1) Charge exchange between positive ions and neutral gas atoms, (2) a less important ionisation by collision by the electrons and the positive ions mostly taking place in a region near the cathode, (3) elastic and inelastic scattering of ions by gas atoms, (4) the formation of a radial, static and space-charge, electrostatic field. Kamke's theory was worked out for a discharge tube of the Lukanow-Schütze type (in which the inter-electrode distance is less than the length of cathode dark space), requires modification when applied to a discharge tube of the usual simple type with the anode placed at a great distance from the cathode. In this case the static radial field is supplied by the positive charges on the glass walls of the discharge tube especially in the region of the cathode dark space (the diffusion current to the walls is predominantly positive as the dominant process of ionisation is considered to be that of electron exchange).

The essential feature of Kamke's theory is that a flat type of radial distribution in the ion-channel changes over into an approximately Gaussian one (the distribution is more accurately shown to be represented by the Hankel function[4]) on account of the effect of scattering and of the radial field. Due to the exchange process there is a continuous replacement of fast ions by the slow ions as the ion-channel proceeds towards the cathode. From the point of view of the theory, it is essential to follow the radial distribution of the ions in the channel, in the various regions in the cathode dark space. The methods mentioned above,[1–4] which measure the radial distribution of the ions at the cathode surface, do not enable such a study to be made. We have therefore carried out a direct measurement of the radial distribution of the light intensity in the discharge channel with a microphotometer, after photographing the discharge channel. The observed luminosity in the dark space (under conditions of the normal discharge) is due to excitation by electrons[1a] but under conditions of the abnormal discharge (since the electrons do not contribute appreciably to the ionisation in the dark space), it is due to the excitation by positive ions and by neutral atoms with and without the charge transfer process. In any case the radial distribution of the light intensity will be a measure of the radial distribution in the electron channel or the positive ion-channel which both mean the same thing because the electron emission from the cathode is predominantly positive-ion dependent. As the ratio, axial/radial electrostatic field in the dark space is large, it is possible to assume as an approximation, that the energy distribution amongst the electrons and the positive ions does not vary in the radial direction.[5]

2. The present paper describes results obtained for discharge in air at voltages, varying from 1·18 kV. to 9·8 kV., discharge current 1·0 m.a., in a discharge tube (of diameter 3·5 cm.). The experimental arrangements employed are those that have been already described.[2]

From the microphotometer records (Figs. 1, 2, 3) it is clear that at lower voltages the ionic distribution is not Gaussian but shows a flat maximum of the type observed by Chaudhri and Baqui.[3] It is only for voltages greater than about 6 kV. that the distribution begins to approximate to the Gaussian, observed by Chiplonkar[2] and Kamke.[4]

In case where the fit with the Gaussian is good, one can calculate how the half width radius (H.W.R.) of the beam varies with z, the distance from the cathode.

TABLE I

Variation of H.W.R., with Distance z, from the Cathode

(Discharge in air, 9·8 kV., 1·0 m.a., length of cathode dark space = D.S.L. = 55 mm.)

z (mm.)	3	8	15	25	35	44·5
H.W.R. (mm.)	18·0	19·3	22·1	28·1	..	..
Remarks ..		Gaussian			Non-Gaussian	

The results show the increase in the localisation as the ion-channel approaches the cathode, as expected from the theory.

Figure 4 shows the plot of J_0/J as a function of r^2 for $z = 8$ mm., and 44·5 mm., assuming an empirical expression for the distribution of the current density $J = J_0 \exp(-h^2r^2)$.

The results given in Figs. 1, 2, 3 support the theory that a flat type of distribution changes over into the Gaussian, on account of the processes occurring in the cathode dark space. This is also well shown by Fig. 3 which gives the variation of the distribution with z for discharge voltages of 2·01 kV., where the distribution however is not Gaussian. It has been observed by us that in cases where the overall fit with the Gaussian is not satisfactory there is always a central axial region over which it can be represented by the Gaussian. The size of this central region ($r \sim 10$ mm.) increases with increase in voltage and with decrease in z.

For voltages below 6·0 kV., where the distribution is non-Gaussian, it is instructive to follow the change in the distribution by observing the variation in the width of the maximum (x) with (z).

The results in Table II again support in general the conclusions drawn from Kamke's theory. One significant result that requires explanation is the increase in the cross-section of the luminous discharge channel in the immediate vicinity of the cathode. A new factor operating in this region is the excitation of atoms by slow electrons released from the cathode. Fig. 5 shows some typical photographs of the discharge channel. The cathode is on the left and the luminous canal ray beam can be seen in one case.

3. The effect due to the elastic and the inelastic scattering by gas atoms can be demonstrated by observing the radial distribution of the light

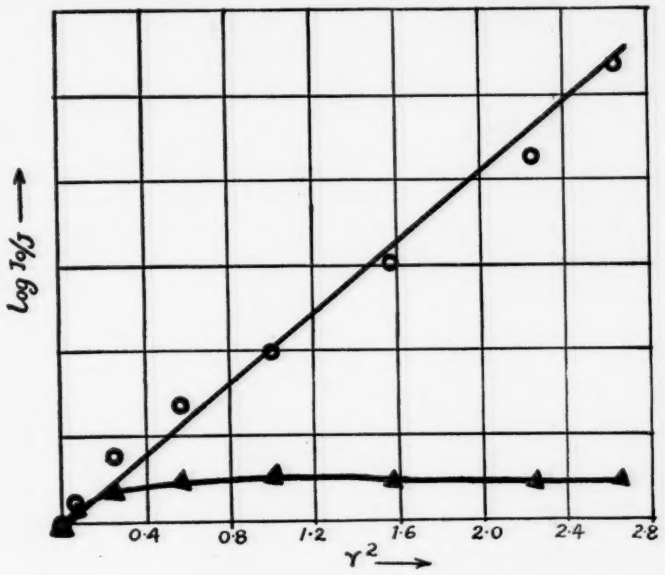

FIG. 4. log J_0/J against r^2. O $z = 8$ mm. ▲ $z = 44{\cdot}5$ mm.

TABLE II

Variation of average width of the maximum (x) *as a function of* (z)

(1) z = distance from cathode in mm.
(2) x = width of maximum in mm. (± 2 mm.).
(3) D.S.L. = length of cathode dark space in mm.
(4) Discharge current = 1·0 m.a.

z = (mm.)		3	8	15	25	35	44·5	55
D.S.L. ↓ mm.	H.T. ↓ kV.	Width of the central maximum in mm.						
18	1·18	13·8	11·8	..	..	..	..	..
30	2·01	12·2	11·2	11·5	14·2	..	..	..
50	6·14	5·7	5·5	5·0	4·7	5·2	..	..
55	9·8	5·7	5·0	4·2	4·5	4·4	6·2	..

intensity in the luminous canal ray beam in the observation chamber which is field-free. The effects here operating are those due to the electron exchange and the scattering and to some extent due to the geometry of the canal.

Figure 6 gives the microphotometer records for the positive ray beam for discharge in air (5·32 kV., 1·0 m.a., D.S.L. = 48 mm.). It has been found that the distribution cannot be represented by the Gaussian. One may therefore measure the width of the maximum as a function of z (in the same way as was done in the previous case) where z now stands for the distance from the cathode as measured in the observation chamber.

TABLE III

Variation of width of maximum (x) *with* (z)

z = mm.	0	3	6	9	12	15	18	21
H.T. 2·63 kV.	0·375	0·416	0·541	0·583	0·458	0·458	0·541	mm. 0·500
5·32 kV.	..	0·646	0·638	0·758	0·638	..	..	..

These results follow more or less the pattern shown by the results obtained for the luminous discharge channel in the dark space given in Table II. From the fluctuations in the cross-section of the discharge channel, it appears that the increase in the cross-section observed in the vicinity of the cathode may not have a simple explanation in terms of the low velocity electrons which are present in the region.

We thank Prof. Asundi for many helpful discussions and suggestions.

REFERENCES

1. *Handbuch Der Physik*, 1956, **22**, 94.
1 (*a*). *Ibid.*, 1956, **22**, 96.
2. Chiplonkar, V. T. .. *Proc. Ind. Acad. Sci.*, 1940, **12**, 440; *Ibid.*, 1947, **25**, 453.
3. Chaudhri, R. M. and Baqui, M. A. *Proc. Phys. Soc.* (*Lond.*), 1952, **65 B**, 324.
4. Kamke, D. .. *Zeits. f. Physik.*, 1950, **128**, 212.
5. Yarnold, G. D. and Holmes, S. *Phil. Mag.*, 1936, **22**, 988.

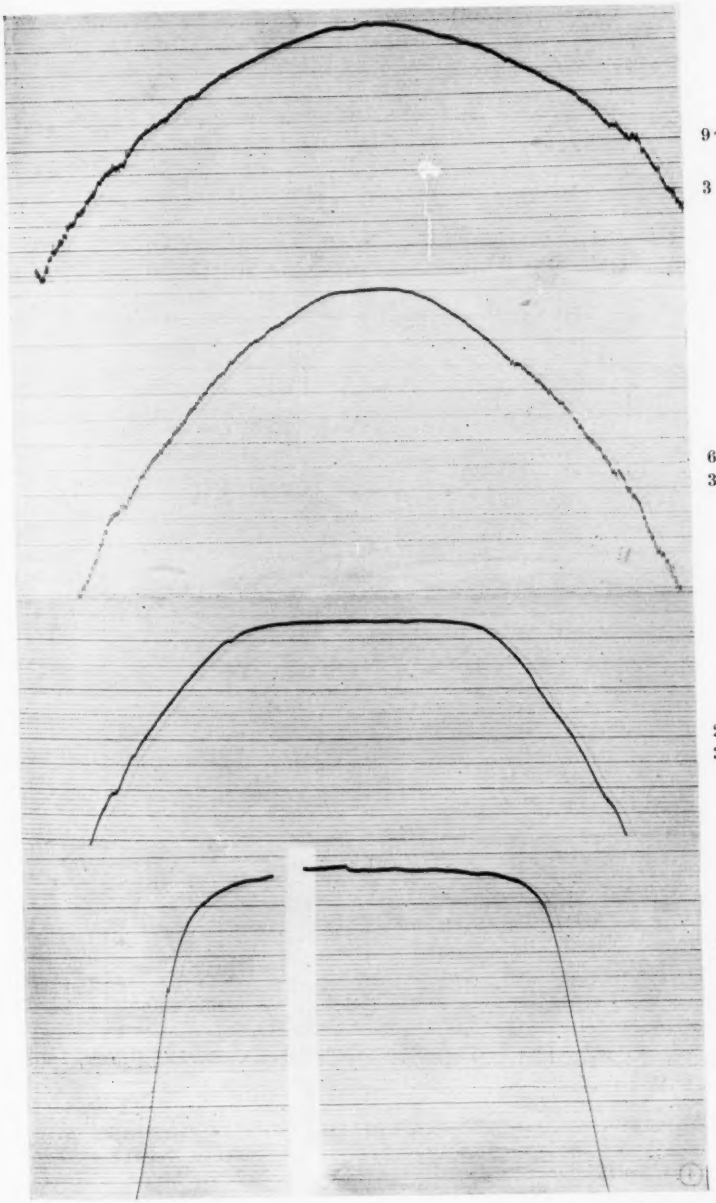

FIG. 1. Variation of the radial intensity distribution with voltage. Discharge in air, 1·0 m.a. $z = 3$ mm., 9·8, 6·14, 2·01, 1·18 kV. Microphotometer magnification, ×4.

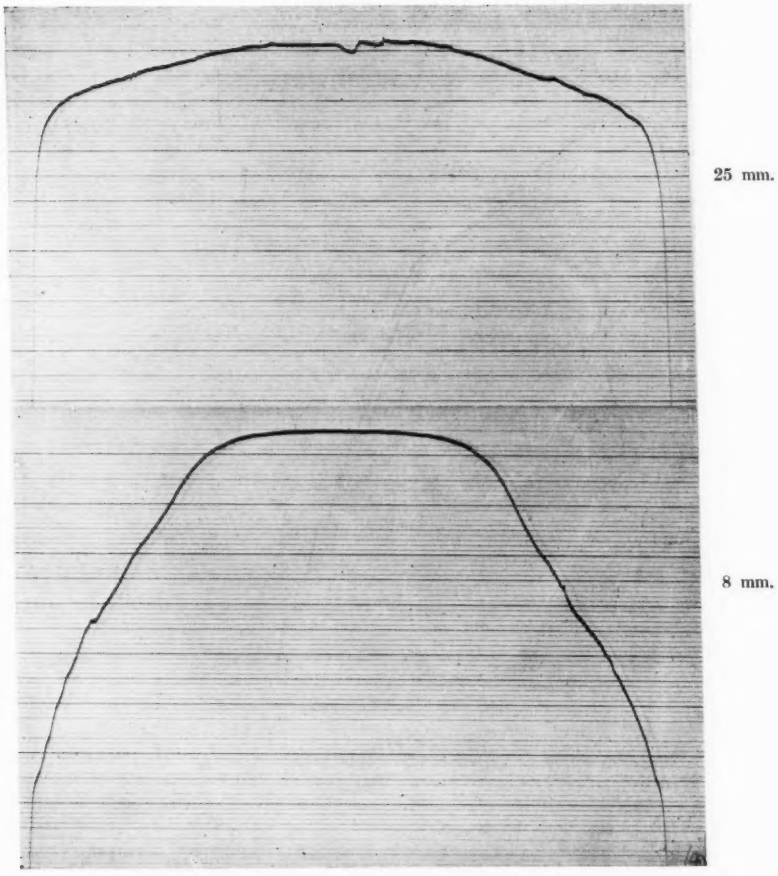

FIG. 2. Variation of the radial intensity distribution with distance. Discharge in air, 2·01 kV., 1·0 m.a., $z = 25$, 8 mm. Microphotometer magnification, ×4.

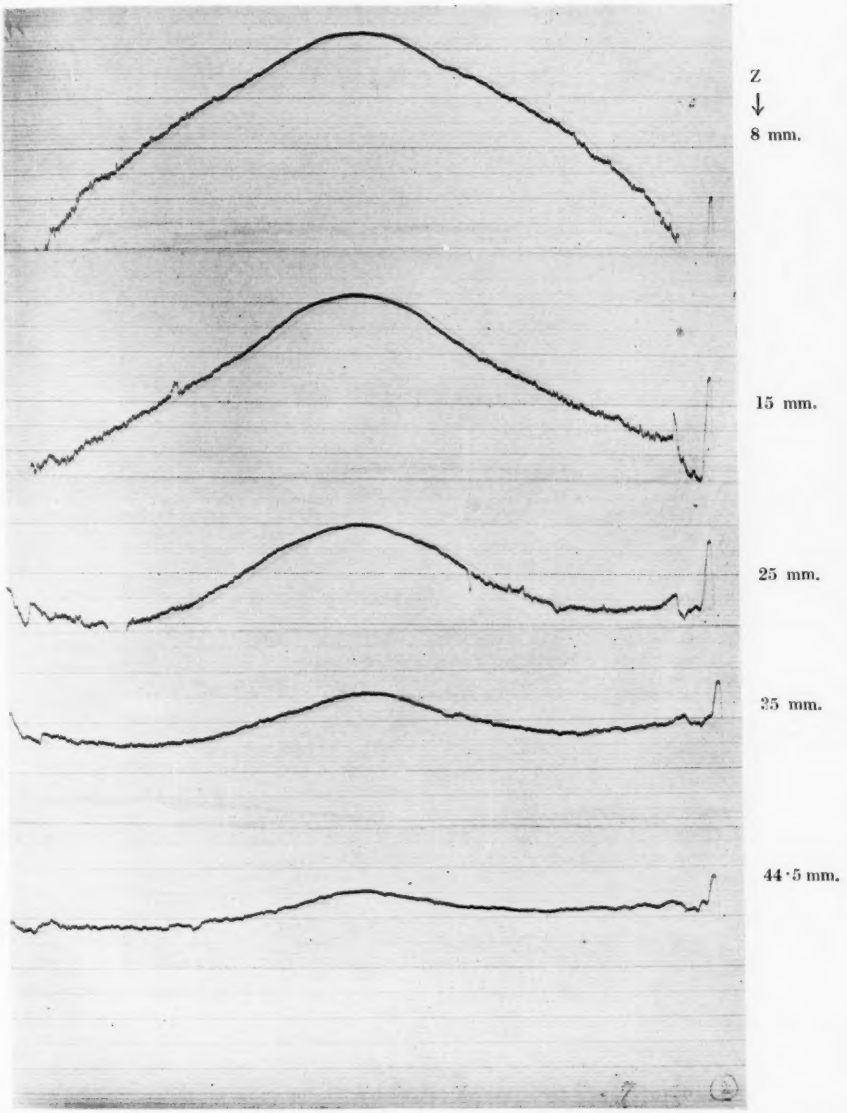

FIG. 3. Variation of the radial intensity distribution with distance. Discharge in air, 9·8 kV., 1·0 m.a., $z = 8, 15, 25, 35, 44{\cdot}5$ mm. Microphotometer magnification, ×4.

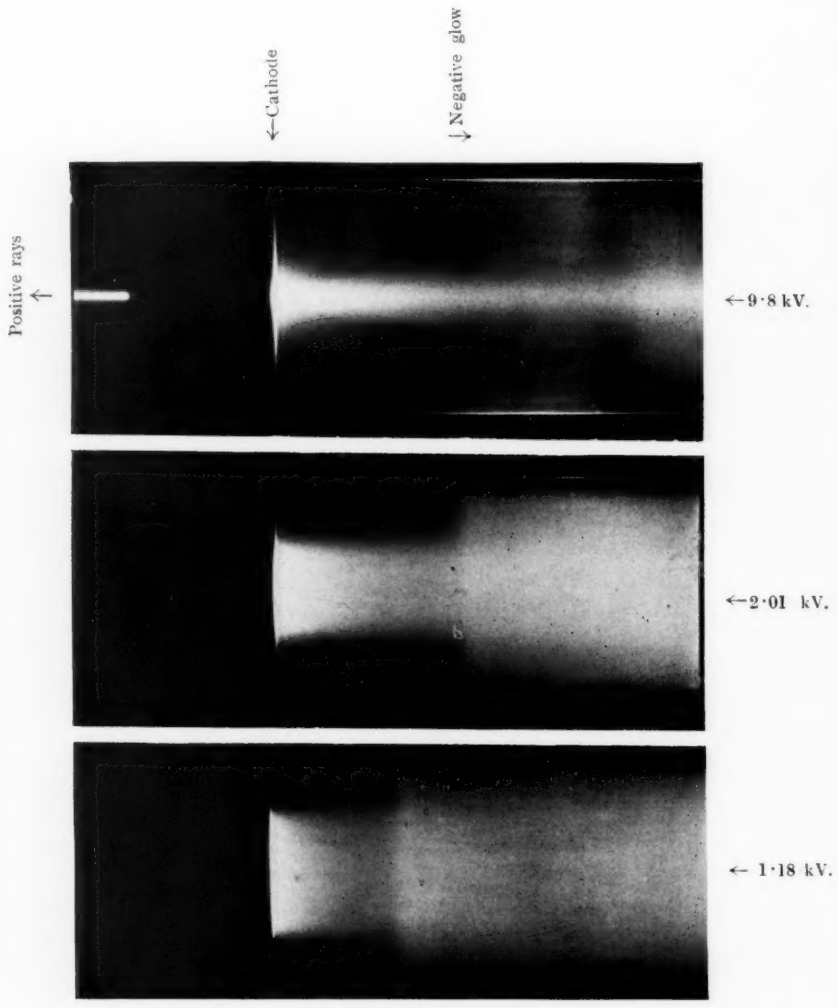

FIG. 5. Photographs of the discharge channel, in air 1·0 m.a. Magnification, ×1.

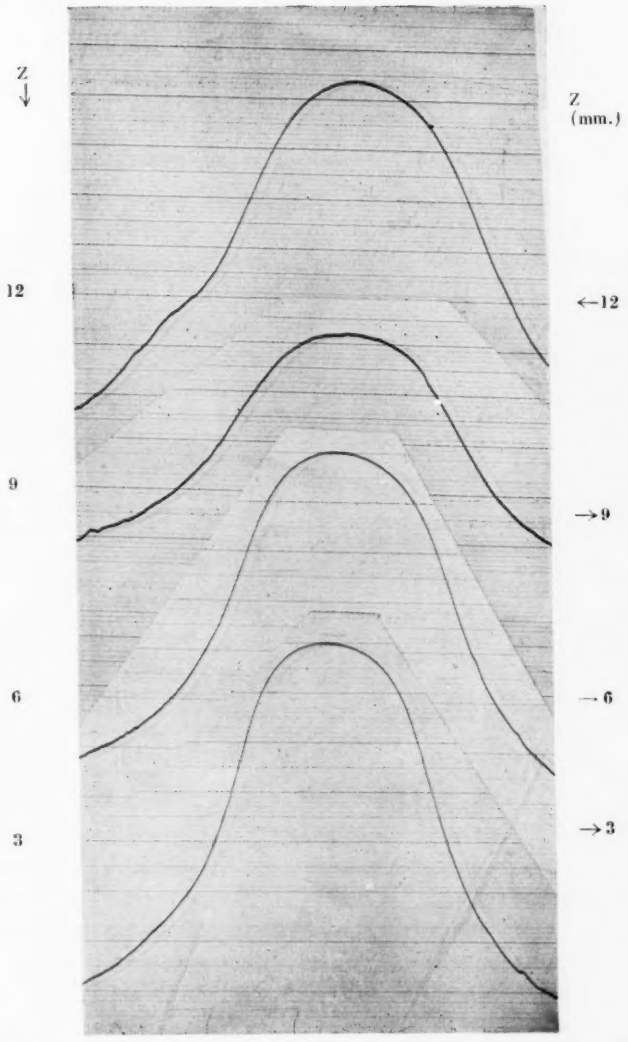

FIG. 6. Radial intensity distribution in the luminous canal ray beam in the observation chamber. Discharge in air 5·32 kV., 1·0 m.a. Microphotometer magnification, ×24.

HETEROCYCLIC COMPOUNDS

Part X.* Synthesis of 14, 15, 16, 17-Tetrahydro-16-Keto-17-Aza-Cyclopenta-(*a*)-Phenanthrene and Substituted 1-Cyclopenta-(*c*)-Quinolines

BY S. KANTHAMANI

(*Department of Organic Chemistry, University of Madras, Madras-25*)

Received August 28, 1957

(Communicated by Dr. K. N. Menon, F.A.SC.)

CLEMO AND MISHRA synthesised 15, 16-dihydro-11-aza-cyclopenta-(*a*)-phenanthrene by condensation of α-naphthylamine with ethyl-2-oxo-cyclopentane carboxylate followed by ring closure and reduction. In the present work an extension of Clemo's work is reported as a preliminary study to a more extensive study in the field of aza-steroids. Ortho- and para-anisidines, para- and meta-toluidines, and β-naphthylamine were condensed with the keto-ester and then ring closed.

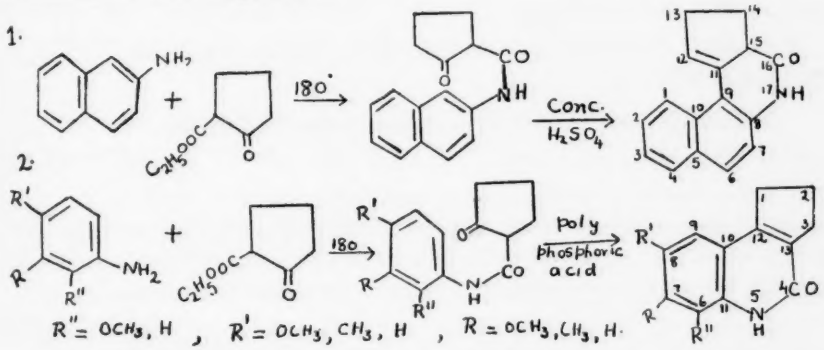

The naphthalide, which gave a blue colour with ferric chloride, was readily obtained, but the anisidides and toluidides were formed only on prolonged heating of the components. Cyclisation, using concentrated sulphuric acid, proved successful only in the case of the naphthalide. The action of sulphuric acid on the anisidides and toluidides led to charring and definite products could not be isolated. Cyclisation proceeded smoothly using polyphosphoric acid.

EXPERIMENTAL

2-Keto-cyclopentane carboxy-β-naphthalide.—Ethyl cyclopentane-2-one-1-carboxylate (7 g.), placed in a round-bottomed flask provided with a condensor

* Part IX, *Proceedings*, Vol. XLV, No. 4, A, 1957, page 260.

and heated to 150° in an oil-bath, was treated with β-naphthylamine (5 g.) the amine being added in small lots extending over a period of 5 minutes. After addition was complete, the temperature of the bath was raised to 180° and maintained at that point for half an hour. The cooled product was repeatedly extracted with alcohol and the solid from the extract crystallised from methanol. The naphthalide crystallised in colourless needles, m.p. 152°, yield: 3·5 g.

Found: C, 76·6; H, 5·8; N, 5·6. Theory $C_{16}H_{15}NO_2$: C, 76·0, H, 6·0; N, 5·5.

14, 15, 16, 17-*Tetrahydro*-16-*keto*-17-*aza-cyclopenta*-(a)-*phenanthrene*.—The above naphthalide (2·5 g.) was added gradually to cooled concentrated sulphuric acid (3 ml.) with stirring. After the initial exothermic reaction had subsided, the mixture was heated on a steam-bath for 15 minutes. The resulting deep brown viscous liquid was carefully poured into ice-water and the resulting solid collected. The aza-ketone was crystallised first from acetic acid and then methanol when 1·5 g. of the pure product, partly decomposing at 300°, was obtained.

Found: C, 81·5; H, 5·5; N, 5·8; Theory $C_{16}H_{13}NO$: C, 81·7; H, 5·53; N, 5·96.

2: 3-*Dihydro*-4-*hydroxy*-6-*methoxy-cyclopenta*-(c)-*quinoline*.—R = R′ = H
R″ = OCH_3

The *o*-anisidide, from 6 g. of cyclopentanone carbethoxylate and 5 g. of *o*-anisidine, crystallised from ethanol in colourless crystals of m.p. 155°. In this condensation, as well as in the case of all the other amines, the heating at 180° had to be continued for 5 hours to complete the reaction.

Found: C, 66·6, H, 6·5; N, 6·2. Theory $C_{13}H_{15}NO_3$: C, 66·9; H, 6·4; N, 6·0.

The *o*-anisidide (3 g.) was added to polyphosphoric acid under cooling. After heating for 5 hours on the steam-bath, the heating was continued at 120 for 2 hours in an oil-bath. The cooled syrupy liquid was poured on to ice and the phosphoric acid neutralised with sodium bicarbonate. The resulting fluffy mass was collected and crystallised from dilute ethanol, m.p. 295-300°, 2 g.

Found: C, 72·18; H, 6·22; N, 6·43. Theory $C_{13}H_{13}NO_2$: C, 72·56; H, 6·01; N, 6·51.

2: 3-*Dihydro*-4-*hydroxy*-8-*methoxy-cyclopenta*-(c)-*quinoline*.—R = R″ = H
R′ = OCH_3

p-Anisidine (5 g.) gave 4·5 g. of the anisidide of m.p. 133°.

Found: C, 67·4; H, 6·4; N, 5·8. Theory $C_{13}H_{15}NO_3$: C, 66·9; H, 6·4; N, 6·0.

Cyclisation of 2 g. of the *p*-anisidide gave 1·0 g. of a pure product decomposing at 285°, after crystallisation from ethanol.

Found: C, 72·4; H, 6·2; N, 6·3. Theory $C_{13}H_{13}NO_2$: C, 72·6; H, 6·0; N, 6·5.

2: 3-*Dihydro*-4-*hydroxy*-7-*methyl-cyclopenta*-(c)-*quinoline*.—R′ = R″ = H
R = CH_3

m-Toluidine (5 g.) gave 4·5 g. of the toluidide of m.p. 141°.

Found: C, 72·1; H, 7·3; N, 6·1. Theory $C_{13}H_{15}NO_2$: C, 71·9; H, 6·9; N, 6·5.

Cyclisation of 1·5 g. of the *m*-toluidide gave 1·1 g. of the product of m.p. 212° after crystallisation from dilute ethanol.

Found: C, 78·2; H, 6·3; N, 6·9. Theory $C_{13}H_{13}NO$: C, 78·4; H, 6·5; N, 7·0.

2: 3-*Dihydro*-4-*hydroxy*-8-*methyl-cyclopenta*-(c)-*quinoline*.—R = R″ = H
R′ = CH_3

p-Toluidine (5 g.) gave 4·0 g. of the toludide of m.p. 135°.

Found: C, 71·5; H, 7·0; N, 6·4. Theory $C_{13}H_{15}NO_2$: C, 71·9; H, 6·9; N, 6·5.

Cyclisation of 1·5 g. of the toluidide gave 1·0 g. of the product of m.p. 220° after crystallisation from dilute ethanol.

Found: C, 78·1; H, 6·4; N, 6·9. Theory $C_{13}H_{13}NO$: C, 78·4; H, 6·5; N, 7·0.

Summary

The synthesis of aza-phenanthrene and cyclopenta-quinolines is reported.

Acknowledgement

I thank Government of India for a scholarship and Dr. K. N. Menon for guidance.

References

Lemo, G. R. and Misra, L. K. .. *J. Chem. Soc.*, 1953, 192.

Bew, D. G. and Clemo, G. R. .. *Ibid.*, 1955, 1775.

LIGHT PROPAGATION IN ABSORBING CRYSTALS POSSESSING OPTICAL ACTIVITY

By S. Pancharatnam

(*Memoir No.* 102 *from the Raman Research Institute, Bangalore-6*)

Received September 24, 1957

(Communicated by Sir C. V. Raman)

§ 1. Introduction

An excellent though unsuspected example of a biaxial crystal possessing both optical activity and pronounced pleochroism was brought to light—in the shape of certain intensely coloured sectors of amethyst—during certain optical studies on this material. Interference figures of a remarkable nature—to be illustrated and discussed in a later paper—were exhibited by these areas. Indeed, it was the peculiarity of the optical phenomena displayed, which first invited the present investigation on the theory of light propagation in such media—a theory which provides, as we shall see, a simple basis for their explanation. Such a theory has also a more general interest: for instance, the measurement of the rotatory power of a biaxial crystal along an optic axial direction cannot be pursued into the absorbing regions of the spectrum without taking cognizance of its results (§§ 8 and 9*c*).

It has been established that the behaviour of both transparent active crystals (Pockels, 1906; Bruhat, 1930) and inactive absorbing crystals (Pancharatnam, 1955 *a*, *b*; Jones, 1942) may be physically pictured and quantitatively explained by a principle of the superposition of the 'elementary properties' associated with the medium. Thus linear birefringence has to be blended either with optical rotation (circular birefringence) or with linear dichroism—according as we are dealing with the former or latter class of crystals. Following the same geometrical method as was adopted for non-active absorbing crystals (Pancharatnam, 1955 *a*; hereafter referred to as P-*a*) we shall discuss the propagation in an active absorbing crystal as due to the superposed effects of linear birefringence, linear dichroism and optical rotation. For any particular direction of propagation, the last-mentioned properties are to be determined respectively, in the usual manner from the corresponding surfaces which characterise the optical properties of the medium; *viz.*, the index- and absorption-ellipsoids (*see* P-*a*, § 2 *a* and § 4 *d*), and the surface of optical rotation. Were this not the case, the method of superposition would have little practical value since the directional variation

of the properties of the medium—as revealed for example in convergent light phenomena—is naturally the most interesting part of the optics of anisotropic media.

It turns out that the two waves that can be propagated along any direction not only possess different velocities and coefficients of absorption, but are in different states of elliptical polarisation, the geometrical forms of which bear no simple relation to one another (§ 4)—except in certain special cases (§§ 7 and 8). The practical advantage of the method of superposition in such a complex case can be properly appreciated only in a later paper, where the principal results are experimentally confirmed. Sections 2–8 deal with media possessing no circular dichroism—the latter being a property which need not be exhibited in all the absorption bands (Lowry, 1935). The results may, however, be expected to apply fairly accurately for all crystals where linear dichroism is visible to the eye—since circular dichroism, even when present, is usually an extremely feeble effect. In § 9 we shall formally include the effects of circular dichroism, using again the principle of superposition.

For the case of absorbing crystals, the method of superposition was first introduced by Jones (1942, 1948) while developing a comprehensive matrix calculus treatment for general optical systems. Jones did not then pursue the method in sufficient detail as to give an overall picture of the optical properties of anisotropic absorbing media. He has, however, recently (Jones, 1956) attempted to correlate his method with the results of the electromagnetic theory; it will be pointed out in a later paper that this portion of his discussion contains an error as far as its applicability to optically active media is concerned.

Pending a more direct theoretical explanation (*see* § 6) as to why the method of superposition works even under the most diverse conditions (Ramachandran and Ramaseshan, 1952; Ramachandran and Chandrasekharan, 1951), its justification in the present instance has to be based on the equivalence of its results with those of the electromagnetic theory of light propagation in active absorbing crystals. The electromagnetic theory will be discussed in a later paper. We may mention that the theory has thus far been solved only for uniaxial crystals (Forsterling, 1912, quoted in Szivessy, 1928).

§ 2. Physical Description of the Method of Analysis

Consider a crystal plate cut perpendicular to an arbitrary direction of propagation Oz, which direction we may with advantage take as being normal to the plane of the paper (*see* Fig. 1 *a*). We first wish to find the states of polarisation of the two plane waves that can be propagated along this direction

(with specific velocities and coefficients of absorption). The principle of the method adopted may be described as follows. Suppose we are given the state of polarisation P, and the phase, of the elliptic vibration incident on the plane z in the medium. Then if the crystal possessed no linear dichroism, the state of polarisation P′ and the phase of the elliptic vibration emerging at the plane $(z + dz)$ could be completely determined from the theory of

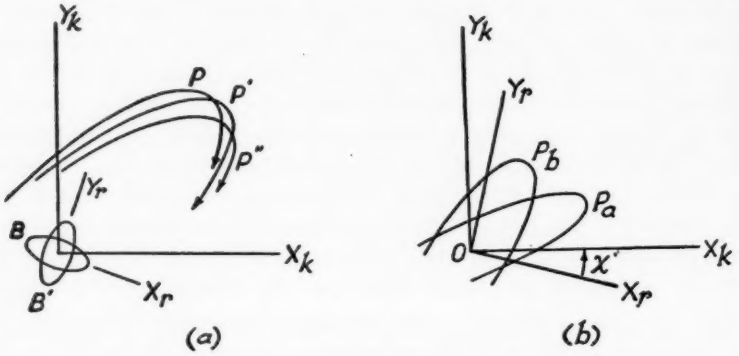

FIG. 1. P—State of polarisation at plane z. P′—State of polarisation at $(z + dz)$ if crystal were transparent. P″—State of polarisation at $(z + dz)$ with linear dichroism also present. P_a, P_b—States propagated unchanged in absorbing active crystal (*i.e.*, states for which P = P″). B, B′—States propagated unchanged in transparent active crystal (*i.e.*, for which P = P′). OX_k, OY_k—States propagated unchanged with linear dichroism *alone* present.

propagation in *transparent* active crystals. Since the crystal possesses linear dichroism, we regard the actual vibration emerging at the plane $(z + dz)$ as obtained by further subjecting the vibration P′ to the following operation of linear dichroism: the vibration P′ is first resolved into its components along the *principal planes of linear dichroism* OX_k and OY_k; the amplitudes of these components are then multiplied by the reducing factors $(1 - k_1 dz)$ and $(1 - k_2 dz)$ respectively, where k_1 and k_2 are the principal absorption coefficients if only dichroism were present. (OX_k and OY_k are parallel to the major and minor axes of the elliptic section of the absorption ellipsoid made by the xy plane.) The operation of dichroism not only causes a diminution in the intensity; because of the differential absorption of the two components the vibration at the plane $(z + dz)$ is now altered to the state of polarisation P″.

In general, however, we shall show that there will be two particular forms of the initial elliptic vibration P for which the vibration P″ at the plane $(z + dz)$ will be in the *same* state of polarisation as the vibration at the plane

z, being therefore altered only in intensity and phase.* These will therefore be the required states of polarisation P_a and P_b of the two waves that can be propagated along the z direction with specific velocities and coefficients of absorption (Fig. 1 *b*).

§ 3. Geometrical Formulation of the Problem

(*a*) *The Poincaré sphere.*—The problem of finding these states of polarisation P_a and P_b permits of an elegant solution if we take recourse to the Poincaré sphere (*see* Fig. 2)—as was done for inactive absorbing crystals (P-*a*). The state of polarisation of any particular elliptic vibration described in the xy plane is represented by a specific point on the surface of this sphere.

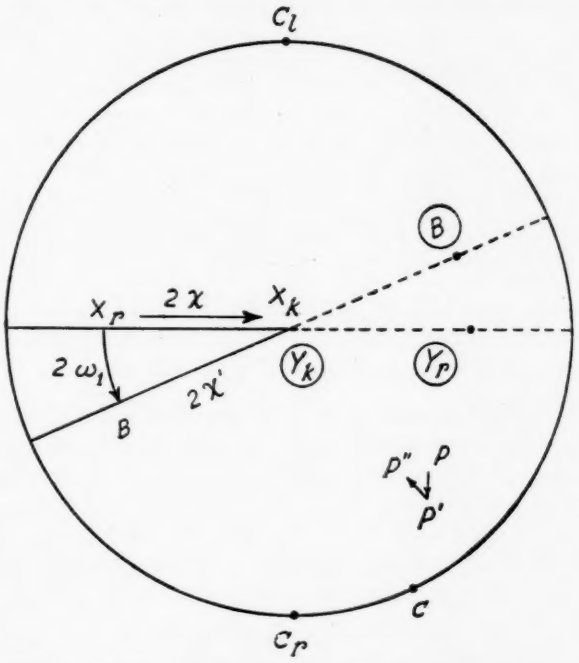

Fig. 2. Representation on the Poincaré sphere of the states described under Fig. 1 *a*. State P′ is obtained from P by a clockwise rotation $\triangle dz$ of the sphere about BB . State P″ is obtained by displacing P′ towards the less absorbed component X_k through a distance $k\,dz \sin PX_k$.

* The sequence in which the two infinitesimal operations are applied is immaterial (if we neglect second order quantities). To prove this, consider the passage of light through a packet made up of infinitesimal lamellæ of two types, the odd members being transparent and the even members absorbing; the effect will not be modified (except to an infinitesimal extent) if the first transparent lamella is removed and placed last.

The definition of the mapping allows the form of the ellipse represented by any point to be directly visualised in terms of the longitude 2λ and the lattitude 2ω of the point; for λ is the azimuth of the major axis and ω the angle of ellipticity.

Thus two linear vibrations along OX_k and OY_k will be represented respectively by two diametrically opposite points X_k and Y_k on the *equator* of the sphere, Fig. 2 being drawn such that the diameter X_kY_k is normal to the plane of the paper. The states of elliptic polarisation of the slower and faster waves that can be propagated in the Oz direction in the absence of linear dichroism will be respectively represented by two diametrically opposite points B and B′. From the theory for transparent active crystals we may regard the oppositely polarised states B and B′ as known, as also the '*elliptic birefringence*' Δ in the absence of linear dichroism, *i.e.*, the phase retardation which the slower wave B suffers *relative* to the other per unit distance traversed.

The relevant results from the theory of propagation in *transparent active crystals* may be briefly recalled. The states B and B′ have respectively the same longitudes as the opposite points X_r and Y_r on the equator which represent the principal planes of linear birefringence OX_r and OY_r (drawn in Fig. 1). Denoting by $2\omega_1$ and $(-2\omega_1)$ the latitudes of B and B′ we have

$$\left.\begin{aligned} \tan 2\omega_1 &= -\frac{2\rho}{\delta} \\ \Delta^2 &= \delta^2 + (2\rho)^2 \end{aligned}\right\} \qquad (1)$$

where ρ is the optical rotatory power for the direction of propagation considered, and δ the linear birefringence, as determined from the index-ellipsoid. The mean of the refractive indices of the waves is the same as in the absence of optical activity (Szivessy, 1928; *see* also § 9 *b* below); *i.e.*, if Δ_1 and Δ_2 be the absolute phase retardations suffered per unit distance by the slower and faster waves, δ_1 and δ_2 being the corresponding values in the absence of optical activity, then

$$\Delta_1 + \Delta_2 = \delta_1 + \delta_2 \qquad (2)$$

(*b*) *Choice of co-ordinate axes in the Poincaré sphere.*—The state of polarisation of the arbitrary elliptic vibration at the plane z (referred to in the previous section) will be represented by a general point P on the Poincaré sphere. We wish to find the condition that the state P should be propagated unchanged. Hence the point P may be most conveniently specified by giving the cosines of the respective angular distances 2ψ, 2ϕ, 2ξ, which it makes with the reference points X_k, B, and a third point C

on the sphere: these points form a right-handed system, the point C being at an angular distance of $\frac{1}{2}\pi$ from X_k and B. (Since the squares of three direction cosines are not independent it is sufficient to specify $\cos 2\psi$ and $\cos 2\phi$ and give merely the sign of $\cos 2\xi$.) The specification of the state of polarisation P by 'direction cosines' is closely analogous to its specification by Stokes' parameters (Fano, 1949; Ramachandran, 1952; Pancharatnam, 1956 *b*). It must, however, be noted that our reference system does not form a rectangular co-ordinate system; the angular distance $2\chi'$ of X_k from B is in general different from $\frac{1}{2}\pi$, and we have

$$\cos 2\chi' = \cos 2\omega_1 \cos 2\chi = (\delta/\Delta)\cos 2\chi \qquad (3)$$

where 2χ is the acute angle between OX_r and OX_k, and ω_1 the ellipticity of the slower vibration B in the absence of dichroism, as given by (1).

(*c*) *Operations of elliptic birefringence and linear dichroism.*—The state of polarisation P'—which would be described at the plane $(z + dz)$ if the crystal were a transparent active one—is obtained from P by an infinitesimal rotation of the sphere about the diameter BB' through a clockwise angle Δdz (Pockels, *loc. cit.*). The infinitesimal movement $\overrightarrow{PP'}$ is therefore perpendicular to the arc BP and has a magnitude ds_R which is equal to $\Delta dz \sin 2\phi$ (*see* Fig. 2). To obtain the actual state of polarisation P'' at the plane $(z + dz)$, we subject the vibration in the state P' to the infinitesimal operation of linear dichroism—whereupon we may expect it to move directly towards the state of polarisation X_k of the less absorbed component, and away from Y_k. It has been proved in a previous paper (Pancharatnam, 1955 *a*, § 4 *b*) that the infinitesimal movement $\overrightarrow{P'P''}$ *is* actually directed along the arc PX_k and has a magnitude ds_k equal to $kdz \sin 2\psi$, where k denotes the 'linear dichroism' $(k_2 - k_1)$.

§ 4. States of Polarisation of the Waves

We wish to find those states P $(2\psi, 2\phi, 2\xi)$ for which the state of polarisation P'' obtained after passage through a thickness dz is identical with P. The condition for this is obviously $\overrightarrow{PP'} = -\overrightarrow{P'P''}$, and this is equivalent to three conditions: (*a*) the magnitudes of the infinitesimal displacements due to elliptic birefringence and linear dichroism should be equal, *i.e.*, $ds_R = ds_k$; (*b*) the displacements $\overrightarrow{PP'}$ and $\overrightarrow{P'P''}$ should be collinear, *i.e.*, from what has been said above, $\angle X_k PB = \frac{1}{2}\pi$; (*c*) the diplacements should be oppositely directed—which means that P is restricted to the hemisphere for which 2ξ lies between 0 and $\frac{1}{2}\pi$. Expressed mathematically the states P

which are propagated unchanged are those for which 2ψ and 2ϕ satisfy the relations:

$$\Delta \sin 2\phi = k \sin 2\psi \tag{4}$$

$$\cos 2\phi \cos 2\psi = \cos 2\chi' \tag{5}$$

together with the condition that $\cos 2\xi$ should be positive.

Let $P_a\,(2\psi_a,\ 2\phi_a)$ represent a state for which 2ϕ is less than $\frac{1}{2}\pi$, and which remains invariant under the operations of elliptic birefringence and linear dichroism (*see* Fig. 3). It is then geometrically evident that the state P_b which makes the same angular distances with the opposite points Y_k and B', will also remain invariant under these operations; this may also be seen from the fact that equations (4) and (5) are unaltered *when* 2ϕ *and* 2ψ *are changed to their supplements*. These states are consequently propagated without change of form. It can be shown that in general there are only two such states, and no more [*see* equations (6) and (7) below]. From the figure it is seen that these states P_a and P_b are represented by two general points on the Poincaré sphere whose longitudes do not in general differ by π and whose latitudes are unequal. We thus arrive at the result that in a medium possessing optical activity, linear birefringence and linear dichroism, *the two polarised waves that can be propagated without change of form along any direction are in elliptical states of polarisation whose geometrical forms bear no simple relation to one another—i.e.*, the major axes of the elliptic vibrations are in general not crossed, their ellipticities are not numerically equal, and they may or may not be described in the same sense. Two polarised states such as P_a and P_b—not being represented by opposite points on the Poincaré sphere—are *non-orthogonally* polarised, and are capable of mutual interference (when coherent) to an extent determined by their 'similarity factor' $\cos^2 \frac{1}{2} P_aP_b$ (Pancharatnam, 1956 *a*). It is seen from the figure that the great circular arc P_aP_b is bisected by C, and hence the (common) third 'direction cosine' $\cos 2\xi$, of the two states acquires an importance as the factor expressing the degree of non-orthogonality of the two states of polarisation.

For the sake of completeness we shall give explicit expressions for the 'direction cosines' of the points P_a and P_b representing the states of polarisation of the two waves. By introducing in (5) the value of $\cos^2 2\psi$ obtained from (4) we obtain a quadratic in $k^2 \cos^2 2\psi$; the positive root of this quadratic (which alone will give a real solution for $\cos 2\psi$) is then found to be given by

$$k^2 \cos^2 2\psi = \tfrac{1}{2}\{(k^2 - \Delta^2) + \sqrt{(k^2 - \Delta^2)^2 + 4\Delta^2 k^2 \cos^2 2\chi'}\} \tag{6}$$

Similarly, eliminating $\cos^2 2\phi$ between (4) and (5)

$$\Delta^2 \cos^2 2\phi = \tfrac{1}{2}\{(\Delta^2 - k^2) + \sqrt{(\Delta^2 - k^2)^2 + 4\Delta^2 k^2 \cos^2 2\chi'}\} \qquad (7)$$

It may be recalled that in these equations $\cos 2\chi'$ is given by (3).

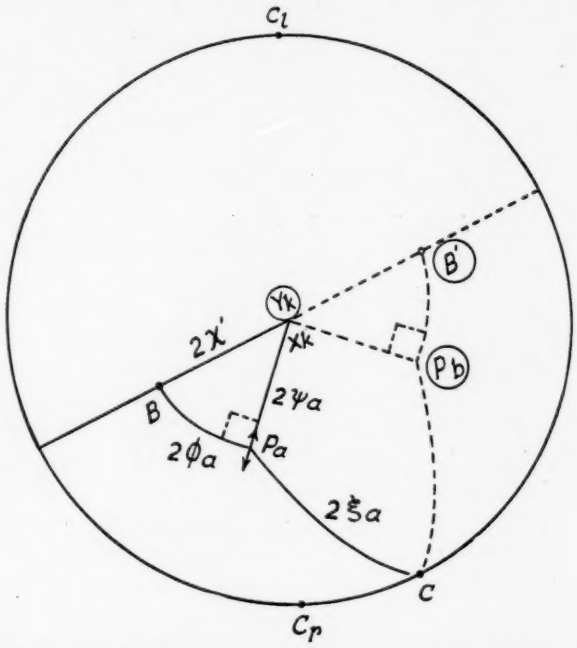

FIG. 3. P_a and P_b represent the states which remain invariant under the operations of elliptic birefringence and linear dichroism described under Fig. 2. The angular distances $2\psi_a$ and $2\phi_a$ of the slower state P_a from X_k and B, are also the angular distances of the faster state P_b from Y_k and B'.

Equation (6) gives two values of $\cos 2\psi$ which differ only in sign, while equation (7) gives two values of $\cos 2\phi$ which again differ only in sign. The corresponding pairs $(2\psi_a, 2\phi_a)$ and $(2\psi_b, 2\phi_b)$ are identified without ambiguity from the condition given by (5) that $\cos 2\phi$ and $\cos 2\psi$ have the same sign if $2\chi'$ lies between 0 and $\pi/2$, while they have opposite signs if $2\chi'$ lies between $\frac{1}{2}\pi$ and π.

The third 'direction cosine' $\cos 2\xi$ is always positive and is the same for both the states P_a and P_b; it is obtained from the first two by the following relation which we shall not prove here.

$$\cos 2\xi = \frac{\sin 2\phi \sin 2\psi}{\sin 2\chi'} \qquad (8)$$

§ 5. Absorption Coefficients of the Waves

The absorption coefficients, k_a and k_b, of the waves in states P_a and P_b may be evaluated exactly as in the case of non-active crystals (Pancharatnam, 1955 *a*). The diminution of intensity $2k_a dz$ which a vibration of unit intensity in the state P_a suffers on travelling a distance dz arises entirely from the operation of dichroism; this operation diminishes the intensities of the X_k and Y_k components of the original vibration by $2k_1 dz \cos^2 \psi_a$ and $2k_2 dz \sin^2 \psi_a$. Hence we obtain, on addition,

$$\left.\begin{aligned} k_a &= \tfrac{1}{2}(k_1 + k_2) - \tfrac{1}{2}k \cos 2\psi_a \\ k_b &= \tfrac{1}{2}(k_1 + k_2) + \tfrac{1}{2}k \cos 2\psi_a \end{aligned}\right\} \qquad (9)$$

so that

$$k_b - k_a = k \cos 2\psi_a \qquad (10)$$

The absorption coefficients have thus been conveniently expressed as functions of the states of polarisation; they may also be otherwise expressed by using the explicit value of $k \cos 2\psi_a$ as obtained from (6). It may be recalled (P-*a*, equation 12) that for any one direction of propagation, k_1 and k_2 are proportional to b_1 and b_2—where $1/\sqrt{b_1}$ and $1/\sqrt{b_2}$ are the lengths of the corresponding principal radii of the absorption ellipsoid.

It is advantageous to anticipate here a small correction to the expression (9) and (10) given later by the electromagnetic theory; if the *extinction* coefficients of the waves be denoted by κ_a and κ_b, then the relations (9) derived by the method of superposition have to be replaced by

$$\left.\begin{aligned} 2\kappa_a v_a^3/c &= \tfrac{1}{2}(b_1 + b_2) - \tfrac{1}{2}(b_2 - b_1) \cos 2\psi_a \\ 2\kappa_b v_b^3/c &= \tfrac{1}{2}(b_1 + b_2) + \tfrac{1}{2}(b_2 - b_1) \cos 2\psi_a \end{aligned}\right\} \qquad (11)$$

Because the velocities v_a and v_b of the waves have been dragged into these new expressions for the absorption coefficients, an exact application of (11) for directions near an optic axis is fraught with difficulty. Luckily for us, however, the error involved in using (9) will be negligible for such directions, since we may set $v_a \simeq v_b \simeq v_m$, where v_m is a mean velocity (*see* P-*a*, equation 14).

§ 6. Refractive Indices of the Waves

We shall next derive expressions for the refractive indices of the waves or, what is virtually the same thing, the respective phase retardations Δ_a and Δ_b which these waves suffer per unit distance of propagation. Our argument is somewhat involved but at the same time illuminating; for it very clearly indicates that the principle of superposition may be derived by regard-

ing the propagation in the medium as due to the forward scattering from induced doublets (*cf.* Jenkins and White, 1937; Kauzmann, 1957).

Let us consider the propagation through a distance dz of a vibration of unit intensity in the state of polarisation P_a. The effect of dichroism consists in diminishing the X_k and Y_k components (whose respective amplitudes are $\cos\psi_a$ and $\sin\psi_a$) by fractions k_1dz and k_2dz respectively. Alternatively the infinitesimal operation of dichroism is equivalent to the operation [which we denote by (*a*)] of *adding* to the original vibration the fractions $(-k_1dz)$ and $(-k_2dz)$ of its X_k and Y_k components. In the succeeding operation of elliptic birefringence the vibration thus obtained is resolved into its components in states B and B′, the phases of these components being then retarded by amounts Δ_1dz and Δ_2dz respectively (where Δ_1 and Δ_2 are the respective phase retardations per unit distance suffered by the two waves in the absence of dichroism). The operation of elliptic birefringence is therefore similarly equivalent to the operation [which we denote by (*b*)] of further adding on the fractions $(-i\Delta_1dz)$ and $(-i\Delta_2dz)$ of the B and B′ components of the original vibration itself (neglecting second order quantities). The occurrence of the imaginary $(-i)$ means that the added vibrations have a phase lag of $\frac{1}{2}\pi$ with respect to the corresponding B and B′ components of the original vibration; the 'amplitudes' of the latter components (that is, the square roots of their intensities) are $\cos\phi_a$ and $\sin\phi_a$ respectively.

But the original vibration in the state P_a is propagated without change of polarisation through the thickness dz under the combined effects of dichroism and elliptic birefringence. Hence—*insofar as its final contribution is concerned*—the effect of dichroism described in (*a*) becomes equivalent to the addition of two infinitesimal vibrations in the *same* state of polarisation P_a as the original vibration: these vibrations are really the resolved components in the state P_a of the corresponding vibrations described in (*a*); they will therefore have amplitudes $k_1dz\cos^2\psi_a$ and $k_2dz\sin^2\psi_a$; but they will be exactly opposed in phase to the original vibration, since only then will they diminish the intensity by $2k_adz$ as given by (9). It follows that the operation of elliptic birefringence (*b*)—*because of its complete formal similarity with* (*a*)—must be effectively equivalent to the addition of two infinitesimal vibrations (whose amplitudes are $\Delta_1\,dz\cos^2\phi_a$ and $\Delta_2\,dz\sin^2\phi_a$) which are in the same state of polarisation as the original vibration, but lag behind in phase by $\frac{1}{2}\pi$. The phase retardation per unit distance Δ_a, suffered by the wave is then equal to $(\Delta_1\cos^2\phi_a + \Delta_2\sin^2\phi_a)$. Or,

$$\left.\begin{aligned}\Delta_a &= \tfrac{1}{2}(\delta_1+\delta_2) + \tfrac{1}{2}\Delta\cos 2\phi_a\\ \Delta_b &= \tfrac{1}{2}(\delta_1+\delta_2) - \tfrac{1}{2}\Delta\cos 2\phi_a\end{aligned}\right\} \qquad (12)$$

where we have used the fact that the mean refractive index in a transparent inactive crystal is the same as when optical activity is also present (Eq. 2). The birefringence is obtained from (12):

$$\Delta_a - \Delta_b = \Delta \cos 2\phi_a \tag{13}$$

When the refractive indices and the birefringence are not required as functions of the states of polarisation, we may introduce in (12) and (13) the explicit value of $\Delta \cos 2\phi_a$ as obtained from (7).

Since the arguments given above are somewhat involved it is worthwhile to indicate how the expression (13) for the birefringence (which alone is of much practical importance) may be *directly* derived. On travelling a distance dz, the alteration of the state of polarisation of any vibration (*e.g.*, from X_k to X_k'), may be evaluated by the method of superposition (as due to linear birefringence alone, in the example quoted). More properly, this alteration is connected with the relative phase retardation $(\Delta_a - \Delta_b)\,dz$ between the two waves (in states P_a and P_b) into which the original vibration will be decomposed; in fact the relative phase retardation must be equal to the area of the infinitesimal quadrilateral $P_a'X_kP_b'X_k'$ (Pancharatnam, 1956 *a*, equation 5 *b*), where P_a and P_b are points opposite to P_a and P_b. The area in question may be shown to be equal to $\Delta dz \cos 2\phi_a$, thus proving (13).

§ 7. CERTAIN SPECIAL CASES

A noteworthy simplification in both uniaxial and biaxial crystals, is that along directions which are nowhere in the vicinity of an optic axis—and where, correspondingly, the linear birefringence δ becomes appreciable—the waves propagated may for most purposes be regarded as linearly polarised along the principal planes of linear birefringence: the reason is that for such directions the ratios (ρ/δ) and (k/Δ) occurring in (1) and (4) usually differ but little from zero. The refractive indices and absorption coefficients of the waves are then obtained from the index and absorption-ellipsoids by the usual constructions (*see* P-*a*, Eq. 12) since we may set $\Delta \simeq \delta$, $\cos 2\phi_a \simeq 1$ and $\cos 2\psi_a \simeq \cos 2\chi$, in (12) and (11).

(*a*) *Uniaxial crystals.*—In uniaxial crystals both the birefringence δ and the linear dichroism k are determined from *uniaxial* ellipsoids; consequently, the ratio (k/δ) is virtually constant for all directions of propagation, and—in accordance with what has been said in the previous paragraph—this ratio will differ negligibly from zero for *all* directions. The states of polarisation of the two waves are then the same as in a transparent active crystal (Eq. 1), since we may set $\sin\phi \simeq 0$ from (4). The refractive indices of the waves, being functions of the states of polarisation (Eq. 12), are also determined as in a

transparent crystal. The waves, however, possess absorption coefficients which are obtained by setting $\cos 2\psi_a \simeq \pm \cos 2\,\omega_1$ in (9), or more accurately, in (11)—the upper sign being chosen if both the index and absorption ellipsoids are of the same sign. The last substitution follows from the fact that in a uniaxial crystal the principal planes of linear birefringence and linear dichroism coincide, so that **B** will have the same longitude either as X_k or Y_k.

(*b*) *Biaxial crystals: directions not too near an optic axis.*—It is known that in both transparent active crystals as well as inactive absorbing crystals the *square* of the ellipticity of the waves may be neglected for directions not too near an optic axis. For such directions of propagation in an active absorbing crystal we shall show that the states of polarisation of the waves are related to each other in the following simple manner. *The major axes of the elliptic vibrations may be taken to coincide with the principal planes of linear birefringence; and the respective ellipticities* ω_a *and* ω_b *of the slower and faster waves will be given by*

$$\left.\begin{aligned}\omega_a &= \epsilon + \omega_1\\ \omega_b &= \epsilon - \omega_1\end{aligned}\right\} \qquad (14)$$

Here ω_1 and $(-\omega_1)$ represent as before the ellipticities of the slower and faster waves in the absence of dichroism alone as given by (1); and ϵ is the common ellipticity of the two waves in the absence of optical activity alone. Neglecting their squares in comparison with unity, ω_1 and ϵ will be given by

$$\omega_1 = -\rho/\delta; \qquad \epsilon = (k/2\,\delta)\sin 2\chi \qquad (15)$$

where χ is the acute angle that OX_k makes with reference to OX_r (measured with the usual sign convention).

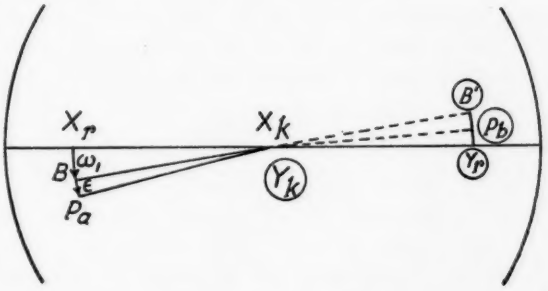

FIG. 4. For directions not in the vicinity of an optic axis each wave has an ellipticity which is the sum of the corresponding ellipticities which would obtain in the transparent active crystal and the inactive absorbing crystal.

For proving these relations we first remark that the directions under consideration are defined by the circumstance that the linear birefringence δ is sufficiently large (compared to both the rotatory power and the linear dichroism) to allow us to neglect the *squares* of (ρ/δ) and (k/δ) in comparison with unity. We may then also set Δ equal to δ according to (1). It follows that in Figs. 2 and 3, the arcs BX_r and $P_a B$ $(= 2\phi_a)$ may both be treated as infinitesimal, since their *squares* may be neglected, according to (1) and (4). The situation is illustrated in Fig. 4 which shows that P_a and P_b have respectively the same longitudes as X_r and Y_r (to our present order of approximation). Also the latitude $2\omega_a$ of P_a is equal to the sum of the *directed* arcs X_rB and BP_a (counted positive if they point to the upper hemisphere). The directed arc X_rB is however equal to $2\omega_1$. Hence for establishing the proposition of the previous paragraph it remains to show that the *directed* arc BP_a must be equal to 2ϵ. This is proved from the following consideration. If in accordance with our approximation we set $2\chi' \simeq 2|\chi|$ and $\Delta \simeq |\delta|$ in (4) and (5), those equations become formally identical with those holding for the case of a *non-active* absorbing crystal (for which case however B coincides with X_r); hence the infinitesimal arc $2\phi_a$ of the present case corresponds to twice the numerical ellipticity of the waves in the non-active absorbing crystal. Moreover, the sign of the directed arc BP_a being opposite to that of 2χ, will be the same as that of ϵ. This proves the first relation in (14) and a similar proof holds for the second relation.

[The approximate expression given in (15) for the ellipticity ϵ of the waves in a non-active absorbing crystal had not been derived in the author's previous paper on the subject (P-*a*). It is, however, immediately obtained either from Eq. (4) of the present paper or from the corresponding equation of the previous paper by setting $\sin 2\phi \simeq 2|\epsilon|$ and $\sin 2\psi \simeq \sin 2|\chi|$.]

The refractive indices and absorption coefficients of the waves may be determined by the usual index- and absorption-ellipsoid constructions, *as though* the waves were linearly polarised. This is because $\cos 2\phi_a \simeq 1$ and $2\psi_a \simeq |2\chi|$ in (12) and (11).

§ 8. PROPAGATION ALONG AN OPTIC AXIAL DIRECTION

In a biaxial crystal the linear dichroism does not in general vanish along an optic axial direction, since the circular sections of the index ellipsoid need not coincide with the circular sections of the absorption ellipsoid. In the absence of linear dichroism, however, the waves will be circularly polarised, so that $\Delta = 2|\rho|$, and the state B coincides with C_r if ρ is positive. The arc $2\chi'$ in Fig. 3 is then equal to a right angle, and from the condition that the angle it subtends at P_a should also be a right angle, it may be seen geometri-

cally [or from Eq. (5)] that P_a must lie either on the meridional arc C_rC ($2\psi = \pi/2$) or the equatorial arc CX_k ($2\phi = \frac{1}{2}\pi$)—as illustrated in Figs. 5 and 6 respectively. Two main cases may therefore be distinguished.

(*a*) *Circular birefringence* 2ρ *greater than linear dichroism* k.—The situation is illustrated in Fig. 5 for the case when ρ is positive (lævorotation).

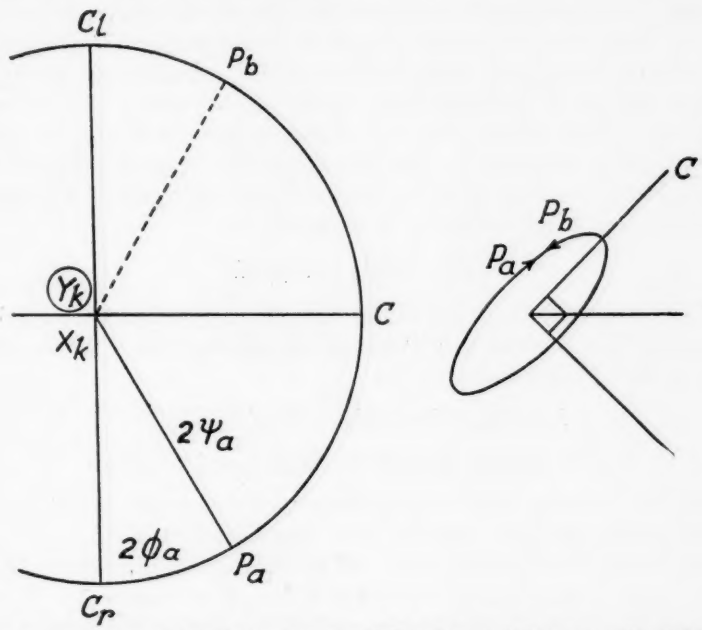

FIG. 5. Discussion of the elliptic states P_a and P_b propagated along an optic axial direction when $2\rho > k$.

Along the optic axis are propagated two elliptic vibrations exactly similar in form and orientation but described in oppsoite senses ($\omega_a = -\omega_b$). The sense of description of the slower elliptic vibration is the same as that of the slower circular vibration which would be propagated along the optic axis in the absence of linear dichroism; the major axes of the two elliptic vibrations are coincident and make an angle of 45° or −45° with reference to OX_k according as ρ is positive or negative. The numerical value of the ellipticity $|\omega_a|$ of the vibrations may be obtained from (4) since $2\phi_a = \frac{1}{2}\pi - |2\omega_a|$, and $2\psi = \frac{1}{2}\pi$.

$$\cos 2\omega_a = k/|2\rho| \tag{16}$$

The two waves have equal absorption coefficients, since $2\psi_a = \frac{1}{2}\pi$ in (10). But they possess different velocities of propagation, the phase retarda-

tion which one wave suffers *relative* to the other per unit distance of propagation being obtained from (13) and (16):

$$\Delta_a - \Delta_b = -2\rho \sin 2\omega_a = +\sqrt{(2\rho)^2 - k^2} \tag{17}$$

(*b*) *Circular birefringence* 2ρ *less than the linear dichroism* k.—Figure 6 illustrates this situation for the case when ρ is positive (the point P_a denotes the state of polarisation of the wave with the smaller absorption coefficient, *i.e.*, for which 2ψ is less than $\frac{1}{2}\pi$). *The waves propagated along the optic axis are linearly polarised, the angle between the linear vibrations being different from a right angle.* The azimuths of the two vibrations with reference to OX_k will be both positive (0 to $\frac{1}{2}\pi$) or both negative (0 to $-\frac{1}{2}\pi$) according as ρ is positive or negative. The numerical value of the azimuths of P_a and P_b (with reference to OX_k) will be ψ_a and $(\frac{1}{2}\pi - \psi_a)$; and if θ be the acute angle between the vibrations, then using (4)

$$\cos\theta = \sin 2\psi_a = |2\rho| \,/\, k \tag{18}$$

The two linearly polarised waves have the same velocity since $2\phi = \pi/2$ in (13). They are, however, propagated with different absorption coefficients as given by (10) and (18):

$$k_b - k_a = k\cos 2\psi_a = +\sqrt{k^2 - (2\rho)^2} \tag{19}$$

§ 9. MEDIA POSSESSING CIRCULAR DICHROISM

(*a*) *The operation of circular dichroism.*—Turning our attention now to the general example of an optically active absorbing crystal, we have naturally to suppose that even in the absence of optical rotation, linear birefringence and linear dichroism (*i.e.*, if we set $\rho = 0$, $\delta_1 = \delta_2 = \delta_m$ and $k_1 = k_2 = k_m$) the waves propagated in the z-direction will be circularly polarised with a difference σ between their coefficients of absorption (left *minus* right), the mean of their absorption coefficients being k_m. We therefore extend the discussion of § 2 in the following manner: the vibration at the plane $(z + dz)$ will now be given by further subjecting the vibration P″ (obtained after the operation of elliptic birefringence and linear dichroism) to the infinitesimal operation of circular dichroism; that is, the vibration P″ must be resolved into its right- and left-circular components, and the intensities of these components multiplied by $(1 - \sigma\, dz)$ and $(1 + \sigma\, dz)$ respectively (the phases being unaltered). It may be easily shown—using the results of a previous paper (Pancharatnam, 1956 *a*, § 6)—that, on the Poincaré sphere, the effect of the infinitesimal operation of circular dichroism will be exactly similar to that of the infinitesimal operation of linear dichroism (considered in P-*a*, § 4 *b*), since exactly the same argument is applicable to both cases; that is, *the state*

P″ will move directly towards the less absorbed circular state C_r, through an infinitesimal arc $\sigma dz \sin C_r P''$.

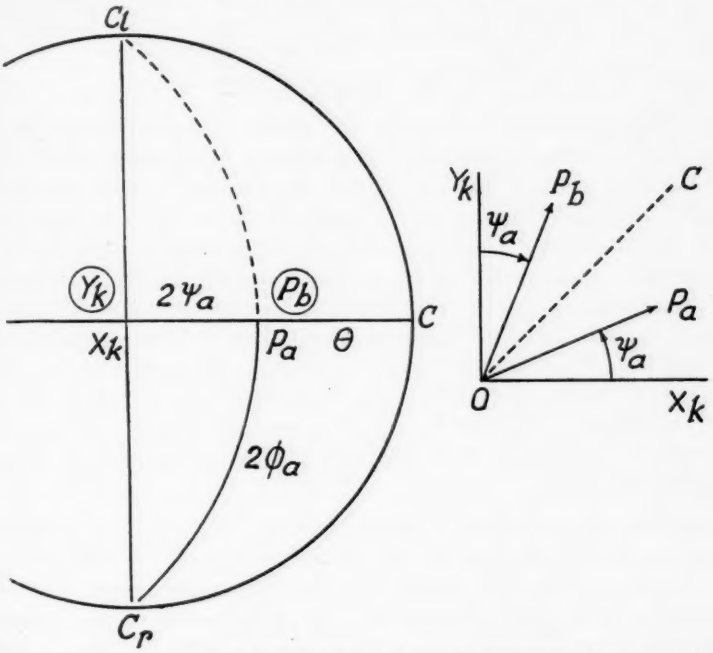

FIG. 6. Discussion of linearly polarised states P_a and P_b propagated along an axial direction when $2\rho < k$.

(*b*) *The superposition of linear and circular dichroism.*—A notable simplification of the analysis is effected by combining first the effects of the infinitesimal operations of linear and circular dichroism alone. [To fix our ideas we may for example consider the propagation along an optic axial direction for a wave-length where the rotatory power becomes zero, the circular dichroism being however near its maximum (Lowry, 1935)].

Just as the infinitesimal operations of linear birefringence and optical rotation (circular birefringence) may be compounded to yield the infinitesimal operation of elliptic birefringence as given by (1), we shall find that *the superposition of linear and circular dichroism results in elliptic dichroism.* More specifically, we shall show that vibrations in two oppositely polarised elliptic states D and D′ (with their major axes along OX_k and OY_k respectively) remain unaltered in form under the combined effects of the infinitesimal operations of linear and circular dichroism (applied in either order); and if

ω_2 be the angle of ellipticity of the less absorbed state D, and K the difference in the absorption coefficients of the vibrations in these two states D′ and D, then,

$$\left.\begin{aligned} \tan 2\omega_2 &= -\frac{\sigma}{k} \\ K &= +\sqrt{K^2+\sigma^2} \end{aligned}\right\} \qquad (20)$$

Consider a vibration initially in one of the states of polarisation D or D′ (*see* Fig. 7, where the diameter $X_k Y_k$ is drawn in the plane of the paper). Under the operation of linear dichroism its state will move towards X_k through a distance $kdz \sin |2\omega_2|$. Similarly, under the operation of circular dichroism the state of the vibration will be displaced towards C_r through an infinitesimal distance $\sigma dz \cos 2\omega_2$. These two movements are oppositely directed whatever be the sign of σ (since ω_2 has the opposite sign) and they will exactly cancel each other since tan $2\omega_2$ is given by (20). Thus vibrations in the respective states D and D′ suffer no alteration in their state of polarisation. The intensities of vibrations in these states will, however, be diminished by specific reduction factors, and correspondingly the absorption coefficients for these two states will have a specific difference K which we proceed to determine.

Consider a linear vibration initially in the state C which lies on the equator at a latitude of $-90°$ with respect to X_k (*see* Fig. 7). Under the operations of linear and circular dichroism its state suffers the successive displacements of kdz towards X_k and σdz towards C_r; in other words, *it suffers a displacement of* $\sqrt{k^2+\sigma^2}\,dz$ *directly towards the state D.* Since however the initial vibration could equally well be considered as the sum of two vibrations (of equal intensity) in states D′ and D, it follows that vibrations in these states suffer no relative phase retardation under the combined operations of linear and circular dichroism; and that the difference in the absorption coefficients of these states is given by the relation (20) which we wished to prove (*see* Pancharatnam, 1956, *a*, § 6).

Moreover, if the initial vibration in the state C be of unit intensity, the diminution of intensity under the operation of elliptic dichroism will be $(K_1 + K_2)\,dz$, where $K_1 dz$ and $K_2 dz$ are the diminution in the intensities of the component vibrations (each with an initial intensity of one-half) in the states D and D′. This diminution of intensity may be equated to that occurring under the combined operation of linear and circular dichroism. Following the same argument as given above, it will be seen that the diminution of intensity arising from the operation of linear dichroism will be $(k_1 + k_2)\,dz$; while the diminution of intensity arising from the operation

of circular dichroism—as described in § 9 *a*—will be zero. Hence, if K_1 and K_2 be the absorption coefficients of the waves which would be propagated in the absence of linear birefringence and optical rotation, then

$$K_1 + K_2 = k_1 + k_2 \tag{21}$$

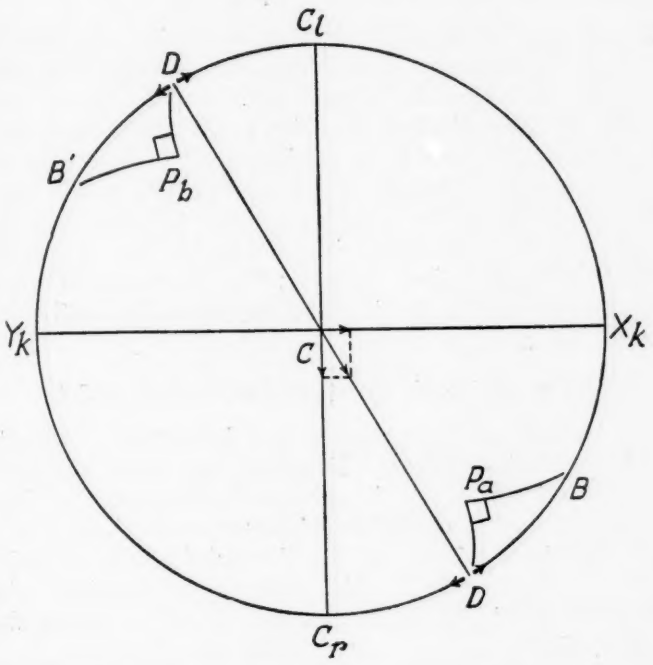

FIG. 7. Illustrating how linear dichroism and circular dichroism may be compounded by a vectorial law to yield elliptic dichroism. P_a and P_b represent the states of the waves propagated along a general direction in a uniaxial crystal possessing circular dichroism.

It has already been shown that the states which remain invariant under the infinitesimal operations of linear and circular dichroism are determined by the same vectorial law which holds for the composition of linear birefringence and optical rotation. Moreover, as in the discussion of § 6, it is easily seen that the infinitesimal operations of linear and circular dichroism are—from the formal mathematical standpoint—completely similar to the corresponding operations of linear birefringence and optical rotation (circular birefringence): the real constants K_1, K_2 and σ occurring in the former case being replaced by imaginary constants $i\delta_1$, $i\delta_2$ and $i\rho$ in the latter case. As a corollary it follows that since the states which remain invariant under the

successive infinitesimal operations of linear birefringence and optical rotation suffer no *absorption*, the states which remain invariant under the successive infinitesimal operations of linear and circular dichroism can suffer no alteration in *phase*. So also, by proving relation (21) above, we have also established the parallel relation given by Eq. (2).

(*c*) *The superposition of elliptic birefringence and elliptic dichroism.*—It will now be clear that along any direction in an optically active absorbing crystal, the effect of elliptic birefringence as given by (1) and (2), has to be combined with the effect of elliptic dichroism [which would be present in the absence of optical activity and linear birefringence, and is given by (20) and (21)]. Correspondingly, it becomes more convenient to specify any point on the Poincaré sphere by its 'direction cosines' with respect to the new reference points D, B and C, which form a right-handed set, and in which only the arc BD differs from $\frac{1}{2}\pi$ (*see* Fig. 8); if we denote arc BD by $2\chi'$, then we will have instead of (3), the following expression for $\cos 2\chi'$ obtained from triangle BDC_1 :

$$\cos 2\chi' = \sin 2\omega_1 \sin 2\omega_2 + \cos 2\omega_1 \cos 2\omega_2 \cos 2\chi.$$

The problem has now been reduced to a form exactly similar to that considered in the previous sections. Hence the states of polarisation of the waves (*specified with reference to the new co-ordinate system*) and the refractive indices and absorption coefficients of the waves are given again by the relations (4), (5), (9) and (12)—except that *the symbol* k *representing the linear dichroism has to be replaced by K* (which represents the magnitude of elliptic dichroism). Because of (21), it becomes unnecessary to replace $(k_1 + k_2)$ in (9) by $(K_1 + K_2)$.

We have thus formally obtained the solution for the propagation in media possessing circular dichroism. For any particular direction of propagation the coefficient of circular dichroism σ is to be determined from the surface of circular dichroism. The media which possess circular dichroism to a striking extent and which at first sight would seem best suited for an easy qualitative test of the theory are certain of the so-called liquid crystals (Voigt, 1916); nevertheless in these liquid crystals, the large 'circular dichroism', the enormous rotation of the plane of polarisation and other phenomena indicate that the medium may not be homogeneous and that, on the contrary, it possesses a lamellar structure (Hl. de Vries, 1951). Since a suitable single crystal was not obtained for experimental study we shall not dwell at any length on the specific results of the theory, but content ourselves with mentioning a few of the results.

For directions which are nowhere in the vicinity of an optic axis the ratio k/Δ and ρ/δ will differ very slightly from zero, so that to a good degree of approximation the propagation will be as in non-active absorbing crystals (*see* § 7). Similarly, if the ratio of the circular to linear dichroism differ very

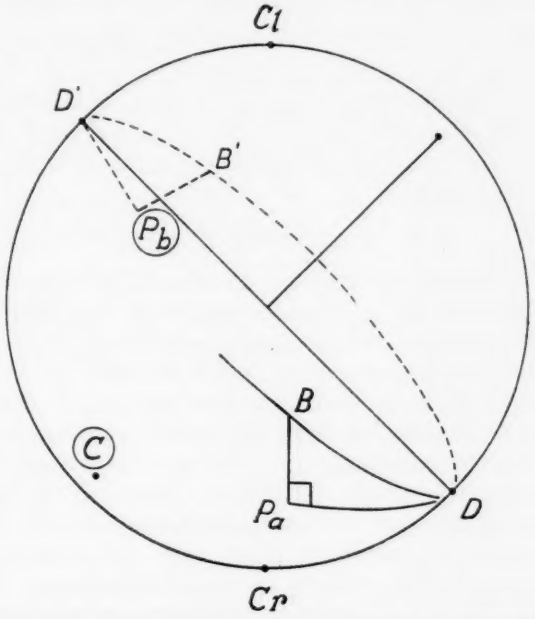

FIG. 8. Propagation in a crystal of the most general class (*i.e.*, possessing circular dichroism also). P_a and P_b represent the states propagated unchanged under the effects of elliptic birefringence Δ (axis BB') and elliptic dichroism K (axis DD').

slightly from zero, as may often be the case in biaxial crystals, we may according to (20) conveniently treat the crystal as though circular dichroism were absent.

For uniaxial crystals, since the principal planes of linear birefringence and dichroism coincide, the points B and D lie on the same great circle passing through the poles. It will then be seen from Fig. 7 that the elliptic states P_a and P_b propagated along any direction bear a simple geometrical relationship to one another; they have the same numerical ellipticity (though they are described in opposite senses); and the orientations of the major axes of the two ellipses are obtained from the principal planes OX_r and OY_r, by turning the latter directions through equal angles in *opposite* directions. This result has been obtained by Forsterling (quoted in Szivessy, 1928) from

the electromagnetic theory of propagation in uniaxial crystals. For directions not too close to the optic axis, the ellipticity of the waves will be the same as in a transparent crystal—since the square of (k/Δ) may be neglected in comparison with unity, so that the arc BP_a is an infinitesimal of the first order and lies along a parallel of latitude.

The states of polarisation of the waves propagated along a general direction in a biaxial crystal will bear no simple relation to one another (*see* Fig. 8); but along the optic axial direction the forms and orientations of the two elliptic vibrations will be simply related to one another—in the same fashion as those propagated along a general direction in a uniaxial crystal (*see* preceding paragraph).

§ 10. CONCLUDING REMARKS

It appears worthwhile to underline the essential difference between our procedure for applying the superposition principle and that customarily followed, *e.g.*, in the case of transparent active crystals by using the Poincaré sphere, or for any crystalline plate by using matrix calculus. The spirit of our method of analysis has *not* been so much to replace the effects produced by an absorbing crystalline plate (on light passing normally through it) by a geometrical or analytical *operation*; it has been to determine the states of polarisation of the two waves that can be propagated along each direction, as well as their velocities and absorption coefficients. This is because the characteristic interference phenomena exhibited by an absorbing crystalline plate, with the incident light partially or completely polarised, is naturally best understood as due to the *interference* and composition of the two non-orthogonally polarised waves emerging from the crystal plate—or their resolved components; in fact this method of analysis is useful for transparent and absorbing crystals alike (*see* Pancharatnam, 1956 *a*, *b*; 1957 *a*, *b*). Moreover, the two waves that can be propagated along any general direction have a physical reality that may otherwise be lost sight of. For example, each will in general have a different ray-direction. [The physical reason for this is that the wave-velocities as given by (12) vary with direction, and in any such medium the direction of propagation of an element of the wave-front will not always coincide with the wave-normal, but may be derived from it by a construction from the wave-surface.] One of the chief merits, then, of the use of the Poincaré sphere is that the states of polarisation of the waves, as well as their velocities and absorption coefficients are determined by extremely simple expressions [(4), (5), (9) and (12)] which remain essentially the same whether the crystal is optically active or not.

The peculiar interference figures exhibited by a sector of amethyst will be explained in detail in a later paper by the application of the method of superposition, so that an overall picture of the optics of such media in the vicinity of an optic axis will emerge. The possibility of the existence of *singular axes*, along which only *one* state of polarisation can be propagated without change of form, will also be investigated. That the properties of the singular axes as described by the method of superposition do not really flout the results of the electromagnetic theory (both in the case of active and non-active crystals) will be indicated in a later paper—which will present the electromagnetic theory of light propagation in active absorbing crystals.

The author is highly thankful to Prof. Sir C. V. Raman for his continued interest in the present investigation.

§ 11. Summary

A light beam in an absorbing crystal may be looked upon as travelling under the superposed effects of the various 'elementary properties' associated with the medium, *viz.*, linear birefringence, linear dichroism, optical rotation and circular dichroism. For any general direction of propagation, this postulate yields completely (*a*) the states of polarisation of the two waves (specified conveniently by two corresponding points on the Poincaré sphere), and (*b*) their velocities and absorption coefficients (expressed conveniently as functions of their states of polarisation). The treatment is closely parallel to that for inactive absorbing crystals (Pancharatnam, 1955)—since for each direction, linear and circular birefringence combine to give elliptic birefringence, while linear and circular dichroism similarly combine to yield elliptic dichroism.

The case of biaxial media with negligible or no circular dichroism is dwelt upon at length. The waves along an optic axis are not circularly polarised: they may even be in two non-orthogonal linearly polarised states (if the dichroism exceed twice the rotatory power). For directions in the near vicinity of an optic axis the waves are in two *elliptic* states of unequal ellipticity with their major axes *not* crossed. For other directions, however, the orientations of the major axes—as also the velocities and absorption coefficients of the waves—become substantially the same as for an inactive absorbing crystal; but the ellipticity for each state now approximates to the sum of the corresponding ellipticities obtaining in the inactive absorbing crystal and the active transparent crystal—thus becoming negligible only when the inclination to both the optic axes becomes notable.

§ 12. REFERENCES

Bruhat .. *Traite de Polarimetrie*, 1930, 319.

de Vries .. *Acta Cryst.*, 1951, **4**, 219.

Fano .. *J. Opt. Soc. Am.*, 1949, **39**, 859.

Jenkins and White .. *Fundamentals of Physical Optics*, McGraw-Hill, 1937, 306.

Jones .. *J. Opt. Soc. Am.*, 1942, **32**, 486.

Ibid., 1948, **38**, 671.

Ibid., 1956, **46**, 126.

Kauzmann .. *Quantum Chemistry*, Academic Press, New York, 1957, 608, 618.

Lowry .. *Optical Rotatory Power*, Longmans, Green and Co., 1935, 393.

Pancharatnam .. *Proc. Indian Acad. Sci.*, 1955 *a*, *b*, **42 A**, 86, 235.

Ibid., 1956 *a*, *b*, **44 A**, 247, 398.

Ibid., 1957 *a*, **45 A**, 402.

Ibid., 1957 *b*, **46 A**, 1.

Pockels .. *Lehrbuch der Kristalloptik*, Teubner, 1906, 309.

Ramachandran .. *J. Madras Univ.*, 1952, **22 B**, 277.

——— and Chandrasekharan *Proc. Indian Acad. Sci.*, 1951, **33 A**, 199.

——— and Ramaseshan .. *J. Opt. Soc. Am.*, 1952, **42**, 49.

Szivessy .. *Handbuch der Physik*, *Band XX*, 1928, Springer, Kap 11, 901, 811.

Voigt .. *Physik. Z.*, 1916, **17**, 159.

THE RATE OF HYDROLYSIS OF CHLOROACETAMIDE IN AQUEOUS ACID

By Sundaresa Soundararajan and Marjorie J. Vold
(*Department of General Chemistry, Indian Institute of Science, Bangalore-3*)

Received September 13, 1957
(Communicated by Dr. K. R. Krishnaswami, F.A.SC.)

Abstract

In 0·3N acid the hydrolysis of chloroacetamide follows a bimolecular law with an activation energy and activation entropy both greater than the corresponding quantities for acetamide in accord with predictions based on the charge distribution. However, at even slightly lower acidity the free energy of activation is a continuous function of the hydrogen-ion concentration becoming more positive with decreasing acidity in the range studied.

This investigation was undertaken in the first instance to find whether the difference in charge distribution within the acetamide and chloroacetamide molecules proposed by Soundararajan[1] to account for their dipole moments would be reflected in a difference in rates of hydrolysis of the C-N bond. The reacting carbon atom was found to carry a formal charge of $+0{\cdot}92 \times 10^{-10}$ e.s.u. for acetamide and $+0{\cdot}73 \times 10^{-10}$ e.s.u. for chloroacetamide. Consequently, a lower activation energy was predicted for the acid catalysed hydrolysis of the chlorine substituted compound.

Hydrolysis reactions which are subject to both acid and base catalysis are usually thought of as involving three distinct reactions, each with its own activation energy and activation entropy according to whether H_3O^+, H_2O or OH^- is the species participating in formation of the activated complex. However, since formation of the activated complex involves removing one of these species from the continuously hydrogen bonded water structure surrounding the dissolved amide molecule and adding it on to the reacting carbon atom to form a transitory pseudo-pentavalent intermediate, it seemed to us possible that the reaction might be describable as a single pseudo-monomolecular process in which, however, the free energy of activation is taken as a function of hydrogen-ion concentration. Hence a second objective was to explore the usefulness or otherwise of this approach.

Since it was desired to know the instantaneous rate of the reaction rather than simply calculating orthodox specific reaction velocities from the integrated form of the usual bimolecular equation, very great care was expended in obtaining precise data.

EXPERIMENTAL

Materials.—Chloroacetamide was prepared as already described by Soundararajan.[1] Sulphuric acid, sodium hydroxide, formalin and all other reagents were of analytical quality.

Procedure.—Weighed samples of the amide were dissolved in 10·0 ml. distilled water contained in thin Pyrex glass bulbs and 20·0 ml. standardised acid of the required strength added from a calibrated pipette while the mixture was chilled and the bulb sealed. Reaction was allowed to proceed for the desired length of time in a water thermostat controlled by a vacuum tube relay, toluene and mercury regulator and both continuous and intermittent heaters to $\pm$ 0·02° C. at 40° C. and $\pm$ 0·03° C. at 50° C. as measured on a calibrated mercury in glass Beckmann thermometer. Twenty to thirty samples including several duplicate pairs were employed at each temperature. At the proper time a bulb was removed, chilled, and its entire contents analysed for ammonium ion by the formal titration method[2] using a Cambridge Research Model pH meter to establish the end points both for back titration of the sulphuric acid originally added and for the base required to neutralise the acid liberated in the formal reaction. Correspondence of the back titration value with the original amount of standard acid taken, to within 0·1 c.c. of 0·1 N base, showed that hydrolysis of the carbon-chlorine bond in chloroacetamide is negligibly slow under the given conditions. This result was confirmed by the virtual absence of free chloride ion only a faint haze being visible upon addition of silver nitrate test solution to the reaction mixture. Measurements were carried out with initial concentrations of amide of about 0·2 N and at two initial concentrations of sulphuric acid, with reaction times extending from 10% to over 80% reaction. Duplicates generally agreed with each other within 0·02% to 0·1%.

Calculations.—For each value of initial amide and initial acid concentration, the concentration of ammonium ion as a function of time was plotted on a large scale so chosen that the curve made as nearly as possible a 45° angle with the co-ordinate axes. Graphical differentiation was then employed to obtain the rates necessary for an explanation of the reaction mechanism.

RESULTS AND DISCUSSION

The detailed results of all experiments are shown in Tables I and II. At 50° the usual bimolecular equation gives a good account of the results up to 45% reaction at all acid strengths investigated. But at 40° a bimolecular law holds only at high acid (0·3 N *vs.* 0·1 N) and only up to 35% reaction. The corresponding specific reaction rates were used to calculate an energy and entropy of activation for comparison with the results of Willems and

Bruylants.[3] For the comparison it was necessary to recalculate their results using the Eyring rather than the Arrhenius formulation.

TABLE I

Rate of hydrolysis of chloroacetamide at* 40° *C.* ± ·02

	dx/dt Moles l^{-1} $sec.^{-1}$ $\times 10^6$	x Moles/l.	$a - x$ Moles/l.	$b - x$ Moles/l.	k_2 Apparent bimolecular specific rate $\times 10^5$	k_1 Apparent monomolecular specific rate $\times 10^6$	% Completion of reactions
1	1·70	0·0296	0·1740	0·2974	3·285	9·76	14·53
2	1·43	0·0402	0·1634	0·2868	3·123	8·74	19·96
							19·54
3	1·38	0·0511	0·1525	0·2759	3·302	9·05	25·08
4	1·09	0·0697	0·1339	0·2573	3·164	8·15	34·25
5	0·71	0·0987	0·1049	0·2283	2·965	6·75	48·45
6	0·47	0·1153	0·0883	0·2117	2·514	5·32	56·62
7	0·51	0·1325	0·0590	0·1945	4·46	8·50†	74·30
							74·20
8	0·185	0·1508	0·0407	0·1762	2·58	4·52	78·68
							78·81
9	0·09?	0·1533	0·0382	0·1737	1·35	2·36†	80·05
							80·09
10	0·592	0·0093	0·1721	0·1296	2·65	3·43	5·146
							5·107
11	0·455	0·0167	0·1647	0·1222	2·22	2·76	9·270
							9·191
12	0·348	0·276	0·1512	0·1113	2·06	2·29	15·46
							15·42
13	0·329	0·0299	0·1489	0·1090	2·03	2·21	16·69
							16·74
14	0·302	0·0333	0·1455	0·1056	1·99	2·07	18·63
							18·61
15	0·285	0·0360	0·1428	0·1029	1·93	1·99	20·16
16	0·258	0·0390	0·1424	0·0999	1·81	1·81	21·57
							21·53
17	0·241	0·0405	0·1409	0·0984	1·73	1·71	22·27
							22·36

* x is the concentration of ammonium ion, $a - x$ unreacted amide, $b - x$ unreacted hydrogen ion. Even at the lowest acidity dissociation of the chloroacetic acid is very small.

† These points correspond to sections of the plot of x *vs.* t from which precise determination of dx/dt is not possible. They have been omitted from Fig. 1.

The activation energy for the acid hydrolysis of acetamide is 17·5 Kcal./mole. For chloroacetamide with its lesser positive charge on the reactive carbon atom the activation energy is lower being 16·1 Kcal./mole. The

TABLE II

Rate of hydrolysis of chloroacetamide at 50° C. ± 0·03°*

	dx/dt Moles l^{-1} $sec.^{-1}$ $\times 10^6$	x Moles/l.	$a-x$ Moles/l.	$b-x$ Moles/l.	k_2 Apparent bimolecular specific rate $\times 10^5$	k_1 Apparent monomolecular specific rate $\times 10^5$	% reaction
1	2·56	0·0531	0·1266	0·2739	7·383	2·12	29·55
							29·52
2	2·11	0·0690	0·1107	0·2570	7·415	1·90	38·41
3	1·66	0·0842	0·0955	0·2328	7·467	1·74	46·82
							46·90
4	1·22	0·0998	0·0799	0·2272	6·72	1·53	55·52
5	0·650	0·1298	0·0499	0·1972	6·61	1·30	72·24
							72·18
6	0·370	0·1430	0·0367	0·1840	5·35	0·981	79·60
							79·60
7	1·28	0·0257	0·1540	0·1132	7·432	0·832	14·3
8	1·12	0·0347	0·1450	0·1042	7·413	0·773	19·28
							19·36
9	0·098	0·0422	0·1375	0·0967	7·371	0·712	23·45
							23·50
10	0·081	0·0547	0·1250	0·0842	7·696	0·650	30·45
11	0·048	0·0753	0·1045	0·0637	7·19	0·458	41·77
							42·17

* x is the concentration of ammonium ion, $a-x$ unreacted amide, $b-x$ unreacted hydrogen ion. Even at the lowest acidity dissociation of the chloroacetic acid is very small.

activation entropies of the two reactions are −55·8 e.u. for acetamide and −54·1 e.u. for chloroacetamide. This difference corresponds to a factor of two in actual reaction velocity whereas the difference in activation energies corresponds to an eight-fold change in reaction velocity.

The reacting system at a molecular level can be considered to consist of the amide molecule surrounded by a cage of solvent molecules to which it may be anchored by hydrogen bonds involving the amine and carbonyl groups. Any of the H_3O^+ groups forming the lining of the cage, that is to say any oxygen atom and three continuous hydrogen atoms from the continuously hydrogen bonded H_2O and acid structure may be the particular one which enters into the reaction. If attention is focussed on one such unit, it can occupy the one position corresponding to formation or incipient formation of the activated complex or $(n-1)$ other positions on the cage lining. Hence the entropy decrease corresponding to transfer from the solvent cage

to the reacting molecule should be larger for a larger value of n. Accordingly the activation entropy is expected to increase somewhat as the internal surface of the solvent cage increases although the effect will be by no means linear. Speculative as it is, this representation is in accord with the experimental fact in the present case and also with the findings of Willems and Bruylants that the " stearic factor " tends to decrease for the sequence of homologous paraffin chain amides as the chain length increases.

Some of the results shown in Table II at 50° and most of the results shown in Table I at 40° do not fit at all to the usual bimolecular formulæ. The bimolecular specific rate declines with increasing extent of reaction or decreasing hydrogen-ion concentration or both. Neither the reverse reaction nor modification of the hydrogen-ion concentration by dissociation of the chloroacetic acid can account for this result. Any side reactions involving the carbon chlorine bond have also been shown to be absent. Uncatalysed molecular reaction with water was also shown to be negligibly slow and incapable of accounting for the results.

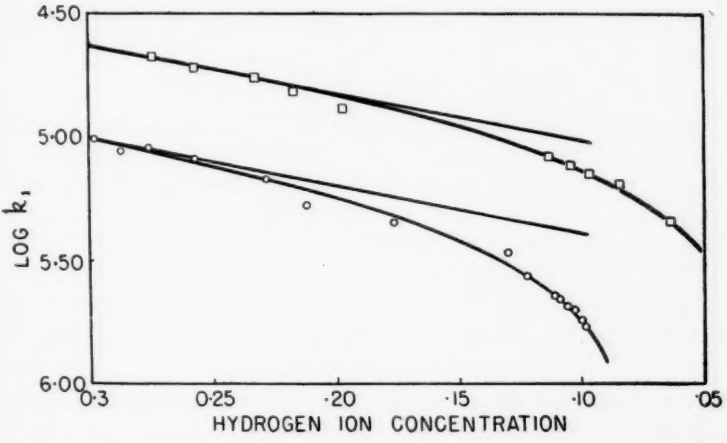

FIG. 1. The plot of the logarithm of apparent monomolecular constant $\left(\frac{dx}{dt}\frac{1}{(a-x)}\right)$ against the hydrogen-ion concentration.

In Fig. 1 the apparent monomolecular constant, $dx/dt \times 1/a - x$ has been plotted against the hydrogen-ion concentration on a semi-logarithmic scale. The plot would consist of two horizontal straight lines for a truly monomolecular reaction and two parallel sloping straight lines for a truly bimolecular reaction. The difference between the two curves is proportional

to the free energy of activation. This quantity increases with decreasing hydrogen-ion concentrations. Thus the hypothesis that the activated complex in this type of reaction may involve the entire cage of solvent molecules rather than some individual water molecule or derived ion, with a free energy of formation varying continuously with the hydrogen-ion concentration appears to be promising.

Further experiments are underway to extend the temperature range and range of hydrogen-ion concentration and further develop the new hypothesis.

The authors wish to record their deep sense of gratitude to Prof. K. R. Krishnaswami for his keen interest in this work.

REFERENCES

1. Soundararajan .. *Trans. Faraday Soc.*, 1957, **53**, 159.
2. Kolthoff and Stinger .. *Volumetric Analysis*, **2**, 158.
3. Willems and Bruylants .. *Bull. Soc. Chem. Belges*, 1951, **60**, 191.

ELECTRO-DEPOSITION AND DISSOLUTION OF ZINC IN ZINCATE SOLUTIONS

By Indra Sanghi* and W. F. K. Wynne-Jones

(Physical Chemistry and Coke Research Labs., University of Durham, King's College, Newcastle-on-Tyne)

Received July 8, 1957

(Communicated by Dr. K. S. G. Doss, F.A.SC.)

Introduction

Technical electroplating of zinc is usually carried out in cyanide, sulphate or phosphate baths. A literature survey pointed out that deposition of zinc from zincate solution is powdery and not very smooth, coherent or adherent. As the problem is very important from the point of view of those alkaline accumulators in which zinc is used, *e.g.*, silver/zinc system, it was considered worthwhile to study the possibility of efficient and reversible deposition of zinc in zincate solutions. A preliminary study of the efficiency and the nature of deposition and dissolution of zinc in zincate solution has therefore been made.

Experimental Technique and Materials

A simple cell of about 100 c.c. capacity, as shown in diagram No. 1, was used. Zinc electrodes ($5 \times 2 \cdot 2 \times 0 \cdot 05$ cm.^{3}) were cut out from sheets which contained a maximum of 0·2% Pb and 0·05% of Cd as impurities. Pt wire was used as auxiliary electrode. Current was drawn from an electronic current stabiliser, employing 10 E.F. 50 valves and an anode voltage of 500 V similar to that used by Thirsk and Wynne-Jones.[1] This instrument was capable of giving a constant current from 100 μA to 100 mA and maintained a stable current even when the output resistance was changed from 0·5 K. to 5 KΩ.

All solutions were made from 'Analar' KOH and ZnO in distilled water and were stored in pyrex vessels. Fresh solution was used for every experiment. However, during the experiment the solution was accessible to air and not stirred.

Polishing and Cleaning the Electrodes

After several trials, the procedure evolved was to smooth out the flat face of the Zn sheet by rubbing down with 6 grades of 'SIA' emery paper

* Present address: Senior Scientific Officer, Central Electro-Chemical Research Institute, Alagappa College P.O., Karaikudi, South India.

(from 0 to 6/0) lubricated with alcohol and rotating the face by 90° between successive grades.

Photomicrograph of the initial unclean surface showed heavy coating of oxide film and patches of oxide while that of the cleaned surface showed a clean shiny surface with the unidirectional ridges due to the final 6/0 emery treatment. Finally the electrodes were wiped with ' Selvyt ' polishing cloth, moistened with alcohol, just before being put in the cell.

STOPPING OFF

The required area, usually 1, 2 or 4 sq. cm., was marked off on the polished flat surface and the rest of the electrode was stopped off with successive coats of polystyrene cement and/or the commercial compound ' Lacomit'.

The cleaned and coated electrodes were initially weighed just before polarization; they were then cathodically or anodically polarized for a known time at a known fixed current, gently taken out, washed with water and alcohol, dried at 60–90° C. and re-weighed.

CALCULATION OF EFFICIENCY

The change in weight of the electrode was assumed to be due to zinc deposited or dissolved by the current and this was used to calculate the " apparent " electrochemical efficiency of deposition by the relation

$$\eta = \frac{\text{observed change in weight}}{\text{calculated change in weight}} \times 100\%.$$

In order to determine the ' true efficiency ' of plating, the electrodes could be brushed by hard bristles, the stop-off removed by solvent (acetone) action and the electrode dried and weighed as before.

Where the procedure of cycling, *i.e.*, anodic or cathodic treatment immediately followed by an equal and opposite treatment under similar conditions, has been used the "apparent" and " net " changes in mass per unit of electrode surface have been given; the " net " changes in mass being calculated thus:

$$\frac{\text{Net changes in mass per cm.}^2}{2 \times \text{No. of cycles} \times \text{No. of coulombs in each anodic or cathodic treatment}}.$$

BLANK TESTS

To make reasonably sure that the electrochemical efficiencies, calculated and expressed as described above, were not made erroneous as the result of any significant chemical attack or interaction between the electrode and electrolyte, blank tests were carried out in which zinc electrodes were left in

2·5-N and 5 N-KOH, saturated with ZnO, for several hours and the change in mass was found to be only a fraction of a milligram even in 4-5 hours.

Results

Cathodic deposition.—It is clear from Table I that the zinc plated out from zincate solutions is loose and uneven. Even a slight improvement

TABLE I

Cathodic deposition of Zn from zincate solutions

Room Temperature about 20° C.

Current density mA/cm.^{2}	Concentration of KOH solutions (Saturated with ZnO)	Apparent efficiency %	Remarks
1	·5 N	50	Shiny, loose, crystallites of Zn sticking to an inner dark layer
	N	104	Same as before
	2·5 N	73	Dark, finely granular and coherent deposit with small nodules
	5 N	20	Same as before
10	·2 N	4	Very thin grey adherent deposit
	·5 N	27	Dark, powdery, but even deposit becoming nodular on prolonged deposition
	N	45	Loose, nodular, uneven, but finely divided, deposit
	2·5 N	89	Similar to above but slightly more even and porous
	5 N	115	A thick white, loose granular and nodular encrustation
50	·5 N	20	Black, adherent finely divided layer
	N	44	Similar to above but nodular
	2·5 N	125	Finely divided but loose and nodular deposit with white encrustation

in coherence is accompanied by a very low electrochemical efficiency. "Apparent" efficiencies of over 100% observed in a few isolated cases are obviously due to the adsorption of electrolyte or the presence of zinc as oxide or hydroxide.

Anodic dissolution.—In Table II are presented the results of experiments dealing with anodic dissolution. The current density and concentration of solution were so arranged, based on our earlier work (under publication separately) on polarization of zinc, as to keep the electrodes either in the "active" or in the "passive" state throughout the duration of the experiment. It was generally found that the electrochemical efficiency of dissolution in "active polarization state" of zinc is above 90% and in the "passive state" below 10%. Only in a few cases were intermediate values for efficiency obtained and this was due to the electrode being active for part of the time and passive for part of the duration of the experiment. In 10 N-KOH, saturated with ZnO, electrochemical polishing occurs.

Anodic-cathodic cycles with zinc electrodes.—In Table III are given the results of cyclic experiments. Again using the information obtained previously the current densities and the electrolyte concentrations were so chosen as to give a high efficiency for individual anodic or cathodic processes. The main inferences drawn from these experiments are:—

(*a*) Better results are obtained if electrodes are first given cathodic rather than anodic treatment.

(*b*) The electrodes generally lose mass on cycling. This obviously is due to the fact that cathodic deposition of zinc from zincate solutions is usually very uneven and loose so that spongy or powdery zinc often falls to the bottom of the cell. In one or two cases where a very slight gain in mass was observed, it may be due to some ZnO or $Zn(OH)_2$ clinging to the electrode surface.

(*c*) When the temperature of the cell was raised (maintained at 50° C.) the apparent loss in weight was often slightly lower, but the true loss in weight remained almost unaltered. It, therefore, appears that although the efficiency of deposition somewhat improves at 50° C., the deposit remains loose and spongy.

Having thus observed that the zincate solutions are alone not quite satisfactory to give adherent and even deposits, suitable surface agents or addition substances were then considered. After some preliminary experiments and rejecting the use of usual surface-active agents for the same reasons as given by Tope,[2] Eckardt's[3] idea of using lead acetate to improve the deposition of

TABLE II

Anodic dissolution of zinc in zincate solutions

Room Temperature about 20° C.

Current density mA/cm.²	Concentration of KOH solutions (Saturated with ZnO)	Apparent efficiency %	Remarks
	·2 N	10	Passivated. Very thin, greyish, adherent and uniform layer
¡	·5 N	83	Unpassivated. Very thin, uniform, adherent, and darkish layer
	·2 N	5	Passivated. Very thin, adherent, black, stain-like layer
	·5 N	17	Same as before
10	N	60	Active first but becoming passivated later. Whitish adherent grey film with black stains on edges
	2·5 N	97·5	Active. Dark grey, uniform film
	5 N	101	Active. Dark grey film with white encrustation on edges
	N	9	Passivated. Dark, jet black, shiny film
50	2·5 N	94	Active; greyish dark film with white encrustation
	5 N	90	Same as above
	N	5·7	Same as above
100	2·5 N	53	Passivated for part of the time. Greyish, brown, powdery film
	5 N	90	Active. Dark film with white encrustation
	10 N	90	Active. Polishing occurs

TABLE III

Cycling of Zn electrodes in zincate solutions

Temperature	Apparent current density mA/cm.²	Conc. of KOH soln. (Saturated with ZnO)	Starting treatment	No. of complete cycles	Duration of each treatment (Mins.)	Observed total apparent change in mass mgm./cm.²	Nett change in mass of electrode in mgm./cm.²	Average change in mass per coulomb per half cycle per sq. cm. of electrode surface (mgm. × 10²)	Remarks
20° C.	10	·2 N	Cathodic	1	50	− 0·4	+ 0·4	+0·66	Black, adherent stainlike surface
			Anodic	1	40	+ 0·5	..	..	Dark, black, coherent and smooth layer
		·5 N	Cathodic	1	50	+ 0·8	+ 0·3	+0·50	Similar to above
			Anodic	1	40	+ 1·6	..	..	Dark, smooth layer but slightly granular
		N	Cathodic	4	40	− 4·0	− 6·2	−3·23	White encrustation ; large amount of powdery zinc falls in cell
			Anodic	3	30	− 4·0	− 8·5	−7·87	Same as above
		2·5 N	Cathodic	4	40	− 4·4	− 9·4	−4·90	Black surface layer with isolated nodules and zinc falls to the bottom
			Anodic	3	30	− 1·7	− 9·6	−8·90	
		5 N	Cathodic	1	50	− 0·3	− 1·2	−2·00	Very thin grayish film
			Anodic	1	40	− 1·7	..	..	White nodular encrustation
		10 N	Cathodic	4	40	− 0·8	− 5·1	−2·66	Black layer with lumps on surface
	50	2·5 N	Cathodic	5	20	−22·9	−24·0	−4·00	Dark surface with white encrustation and isolated grains of zinc, spongy zinc falls to the bottom of cell
		5 N	do.	do.	do.	−22·0	−23·4	−3·90	
		10 N	do.	do.	do.	−24·8	−25·2	−4·20	
	100	5 N	do.	do.	do.	−54·6	−55·7	−4·64	do.
		10 N	do.	do.	do.	−54·0	−57·0	−4·75	
50° C.	50	2·5 N	Cathodic	5	15	−14·4	−15·9	−3·53	Large amount of zinc falls to the bottom and loose, spongy irregular deposit.
		5 N	do.	do.	do.	− 4·0	−11·5	−2·55	Same as above but more coherent appearance and less fall of zinc in cell
		10 N	do.	do.	do.	− 0·5	− 6·5	−1·44	
	100	5 N	do.	5	15	−11·0	−29·0	−3·22	Uneven, thick, loose, spongy, deposit of zinc on lower part of electrode.
		10 N	do.	do.	do.	− 3·0	− 5·0	−0·55	Similar as above but less uneven

zinc from zincate solution was tried. Accordingly, experiments on cathodic deposition and cycling in N, 2·5 N and 5 N-KOH saturated with ZnO were repeated after adding 0·1 gm. of lead acetate per litre of electrolyte. The current densities used this time were 10, 20 and 40 mA/cm.^{2} out of which zinc passivated only at 20 and 40 mA/cm.^{2} in normal electrolyte. The results were interesting and are tabulated in Tables IV and V.

TABLE IV

Cathodic deposition on Zn electrodes from zincate solutions containing 0·1 gm./lit. Pb Ac

Room Temperature (about 20° C.)

Current density mA/cm.^{2}	Concentration of KOH solutions (Saturated with ZnO)	Apparent efficiency %	Remarks
10	1 N	66	Smooth, coherent and whitish grey deposits
	2·5 N	61	
	5 N	81	
20	1 N	45	do.
	2·5 N	76	
	5 N	88	
40	1 N	33	Slightly darker and granular deposits
	2·5 N	70	
	5 N	81	

The zinc plating is greatly improved in appearance and structure by the addition of even slight amounts of Pb as foreign ions, as can be seen from a few typical comparative photographs shown in Plate XVII. At 10 and 20 mA/cm.^{2} specially, the deposits were quite smooth and coherent and at the same time the current efficiency of deposition was also high (about 75%).

On cycling also it was found that the physical condition of the plate even after a prolonged treatment of 15 hours or so showed much improvement as compared to previous experiments, and there was less accumulation of loose Zn granules under the plate in the cell.

During these experiments sometimes a clear and well-defined, coherent and often smooth layer with a tendency to flake, was formed on the electrodes

TABLE V

Cycling of Zn electrodes in saturated zincate solutions containing 0·1 *gm./lit. lead acetate*

Starting treatment cathodic in all cases; Duration of each treatment 30 mins.

Temperature °C.	Apparent current density mA/cm.²	Con. of KOH soln. (Saturated with ZnO)	No. of complete cycles	Observed total apparent change in mass mgm./cm.²	Observed nett change in mass of electrode in mgm./cm.²	Average change in mass per coulomb per half cycle per sq. cm. of electrode surface (mgm. × 10²)	Remarks
20	10	2·5 N	13	−12·5	−27	−5·7	A coherent, uniform layer which tends to flake off from the Zn surface near the edges of electrode
			15	− 9·2	−31	−5·7	
		5·0 N	15	+ 0·5	−12	−2·3	
	20	2·5 N	13	− 40	−73	−7·8	Particles of spongy zinc fall off the electrode
			15		−79	−7·3	
		5·0 N	15	− 8·5	−55	−5·1	
	40	2·5 N	13	− 9·6	−101	−5·4	..
			15	−12·9	−150	−6·9	
		5·0 N	15	− 5·2	−106	−4·9	
50	10	2·5 N	16	− 6	−38	−6·6	..
		5·0 N	17	+ 1·8	−5·5	−0·9	
	20	2·5 N	16	−56·6	−102	−8·9	Loose, spongy zinc with isolated grains
		5·0 N	17	− 6·5	−39	−3·2	
	40	2·5 N	16	− 31	−158	−6·9	Loose deposit with isolated clumps of spongy zinc
		5·0 N	17	− 29	−100	−4·1	

which had been cycled. This flake was attached to the substrate but was quite strong mechanically to be carefully isolated and removed on to microscope slides with the help of a sharp scalpel. Such layers were sometimes removed in this way, weighed in a balance and then studied under the microscope. A typical microphotograph of the layers formed during cycling under different conditions is shown in Plate XVII (*e*). A rough estimate of their thickness showed that it ranged between 3–10 μ.

After ascertaining that the presence of traces of Pb did actually improve the nature of zinc deposition, various attempts were made to find out the part played by lead.

The amount of lead involved was found to be too low to be determined by the usual chemical methods. It was then attempted to use radioactive tracer techniques. Thorium B was tried. The electrolyte used was 2·5N-KOH saturated with ZnO and containing 0·1 gm./lit. of Pb acetate. The solution was rendered active by adding a few c.c. of diluted solution containing Thorium B. Three experiments were performed as follows:—

(*i*) *Liquid count.*—Zn was deposited on 1, 2 and 4 sq. cm. areas at current densities of 40, 20 and 10 mA/cm.^{2} from the same electrolyte in three cells connected in series. After plating, the electrodes were taken out, washed with water and then the plated areas dissolved in 100 c.c. concentrated HNO_3 separately. The solutions were left overnight and then the activity measured by Geiger Counter in the usual manner.

In order to distinguish between the plating of lead or its inclusion in the lattice from that of mere surface adsorption, similar electrodes of 1, 2 and 4 sq. cm. area were placed in the same electrolyte for the same time and then washed and dissolved in 10 c.c. concentrated HNO_3. The activity of these was also similarly counted.

The experiment clearly indicated that:—

(*a*) The activity of the plated zinc, dissolved in HNO_3, was equivalent to the activity of about 5–8 c.c. of the original electrolyte and that it decreased in the following order. Activity of solution of 1 cm.^{2} area plated at 40 mA >activity of solution of 2 cm.^{2} area plated at 20 mA > activity of solution of 4 cm.^{2} area plated at 10 mA current density.

(*b*) The activity of plated electrodes was significantly greater than that of similar blank electrodes placed in the electrolyte without any flow of current. Further, these differences between the activities of plated and blank electrodes decreased in the order given above.

(*c*) The ratio Pb : Zn in the electroplate is increased to about 3 times the ratio in the original electrolyte, *i.e.*, to 1 : 100 in the electroplate from 1 : 330 in the elctrolyte.

(*ii*) *Solid count.*—Three similar electrodes of 2 sq. cm. area were plated at 20 mA/cm.^{2}, as in the previous experiment. But in this case the electrodes after plating and washing were not dissolved in HNO_3 but treated as follows:—

(*a*) The first electrode was dried and its activity measured after 12 hours. (*b*) The second electrode was dipped in dilute inactive $Pb(NO_3)_2$ solution (0·002 M/lit.) for 10 minutes, washed, dried and its activity measured after 12 hours.

(*c*) The third electrode was dipped in concentrated inactive $Pb(NO_3)_2$ solution (0·5 M/lit.) for 10 minutes, washed, dried and activity measured after 12 hours.

This experiment was designed to give an idea of the adsorbed radioactivity as related to the plated lead but was not fully successful as zinc is baser than lead and so large amounts of Pb got deposited on the zinc plate by simple electrochemical replacement as soon as it was dipped in inactive lead nitrate solution. However, it was found that activity decreased in the order of first, second and third electrode respectively. This was in conformity to the expectations.

(*iii*) *Solid count.*—The previous experiment was repeated and this time the second and third electrodes were placed in 250 c.c. of distilled water for 2 and 12 hours respectively. Also, a similar clean electrode was dipped, as a blank test, in the electrolyte for the same time without any passage of current.

This experiment showed that:—

(*a*) The activity due to surface adsorption is negligible.

(*b*) Most of the activity is due to the lead actually being deposited with and on zinc.

(*c*) Even when no current is passed, lead tends to get deposited on the zinc electrode by electrochemical replacement and this often accounts for more than half of the activity found on the plated electrodes.

DISCUSSION

Electro-deposition.—From the above experiments it may be inferred that smooth, even and adherent deposition of zinc is difficult to obtain from pure zincate solutions. But, an improvement can be effected by the addition of

traces of lead acetate to the electrolyte and this improvement is most marked at 10–20 mA/cm.^{2} current densities. Further it is suggested that the improvement in the deposition of zinc may be due to the following reasons:—

(*a*) Formation of a thin layer of lead on the zinc plate by electrochemical replacement as soon as it is dipped in the electrolyte. This may change and influence the basal lattice forces so as to provide better conditions for a more coherent zinc deposition, adherence and crystal growth. Or

(*b*) The removal of the oxide layer, which is known to be present on zinc electrodes, by the local cell action of Pb^{++} ions on the zinc surface. This view finds support in the work of Simmond and Ruder[5] who found that the exchange activity between metals and ions in solutions mainly takes place through the mechanism of local cells. Or

(*c*) Variation in the nature and extent of active areas present on the electrode surface.[6]

In this connection it may be of interest to note the contradiction in the ideas of previous workers as to the efficiency of the presence of Pb^{++} ions, *e.g.*, Morgan and Ralston[7] when using lead electrodes did not observe any specific effect of Pb^{++} on deposition; while Hull and Wernlund[8] attributed the great improvement produced by small amounts of molybdic acid or Mo^{++} to the removal of Pb^{++} from the solution. However, these experiments found that the presence of Pb^{++} improves the nature of zinc electroplate.

Not much change in the polarization or overvoltage was produced by the addition of lead acetate. In fact zinc in 2·5 N-KOH (saturated with zincate) can be efficiently dissolved or deposited at 20 mA/cm.^{2} for less than 100 mV. change from its rest potential. But it is not reversible from the point of view of mass due to the loss in weight of the electrode and its deposition in granular or oxide form on the bottom of the cell.

Titov and Paleolog[9] attributed this to the accumulation of impurities (*e.g.*, carbonate, etc.) which may cause the coagulation of $Zn(OH)_2$ which gets occluded in the plating.

Fundamentally, a good adhesion of electro-deposits can only be obtained when the deposited atoms engage the unoccupied bond energy levels of the outermost atoms of base-metal surface-lattice.

The presence of foregin ions not only prevents deposited atoms from coming within the distances over which the bond energies are effective but also blocks those vacant energy-sites so that they are no longer available to hold and support the electroplated metal atoms. In the case of zinc we are usually faced with two types of surface films:—

(*a*) Porous or discontinuous films which allow the electroplate to penetrate or ' anchor ' in the base-metal only at some points but not continuously or uniformly.

(*b*) Conducting or semiconducting oxide films which cover the electrode surface but allow the metal deposition to occur on top of them. In such cases the oxide films sooner or later break down or peel off under the stresses of electro-deposition.

In both these cases it is inevitable that a poorly adherent plating would be obtained unless extreme precautions are taken. It also explains why acid and cyanide baths often give better adhesion, the reason being that they often dissolve, remove or replace the unsuitable surface oxide films. These ideas are in agreement with those of Lyons.[10]

Electro-dissolution.—The conditions were so chosen as to keep the zinc anodes in active polarization region. It is therefore reasonable to presume that zinc freely goes into solution with an overall efficiency of about 90%. The small deficiency of 10% may be due to chemical precipitation or recrystallisation effects.

The problem of the exact mechanism of zinc going into solution is a very complicated one. However, the following general equations may safely be assumed:—

$$Zn \rightarrow Zn^{++} + 2e$$

$$X\,Zn^{++} + Y\,OH^- + Z\,H_2O \rightarrow Zn_C$$

where Zn_C is the complex zincate ion.

According to Dirkse[11] the value of $X = 1$ and $Y = 4$ in the above equation so that effectively the zincate ion is $Zn(OH)_4^{--}$.

It would have been quite simple and easy if the reaction could be assumed to be directly $Zn + 4\,OH^- \rightarrow Zn(OH)_4^{--} + 2\,e$. But such a reaction involving four electron transfers simultaneously seems very improbable. So, the reaction must proceed through the primary formation of ZnO or $Zn(OH)_2$ which may subsequently react as follows:—

$$ZnO + H_2O + 2\,OH^- \rightarrow Zn(OH)_4^{--} \text{ or}$$

$$Zn(OH)_2 + 2\,OH^- \rightarrow Zn(OH)_4^{--}$$

This view has been supported by Huber *et al.* However, the present state of knowledge is insufficient to give one clear final answer without any ambiguity. But it seems plausible that both the above reactions take part at different stages of anodic polarization. But as far as the deposition and

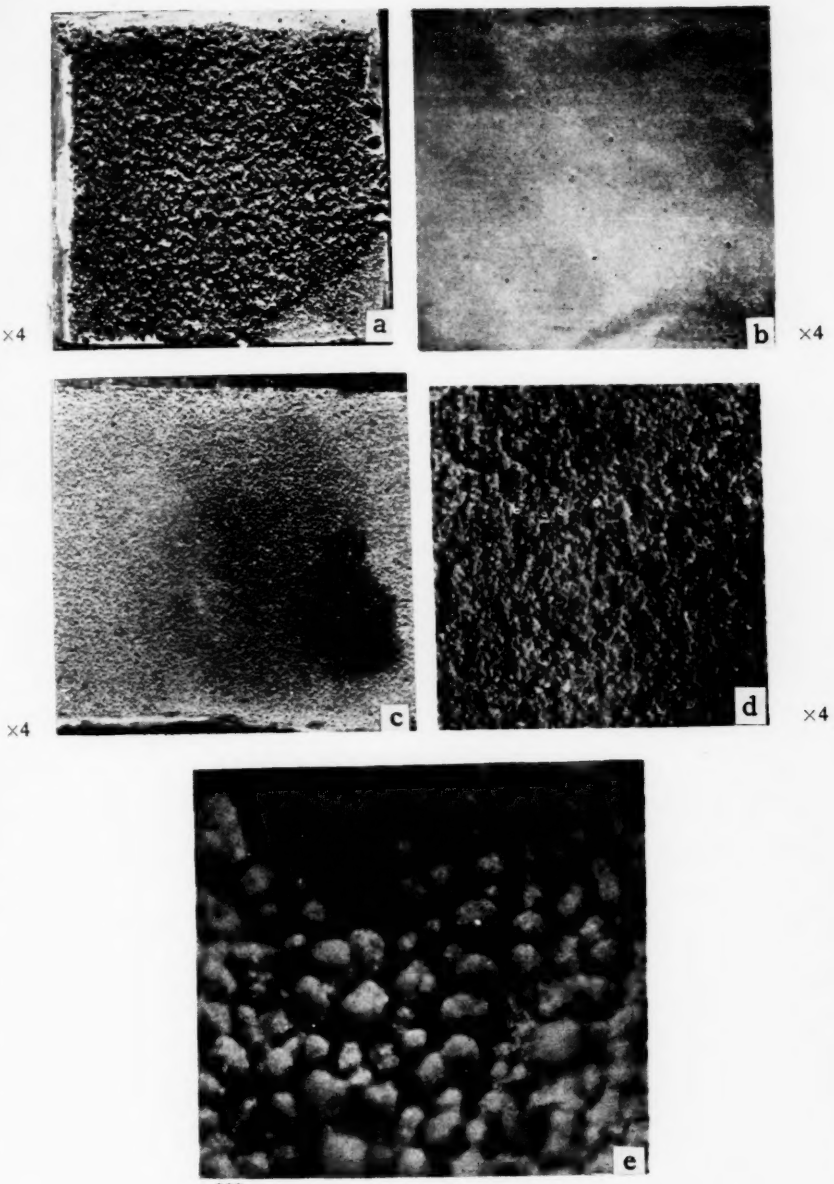

×4 ×4 ×4 ×300

Effect of lead ions on electro-deposits of zinc from zincate baths

(*a*) Cathodic deposition at 10 mA/cm.² in 2·5 N-KOH (saturated with ZnO).
(*b*) Do. with ·1 gm./lit. of Lead Acetate.
(*c*) Zinc electrode after 1 cycle at 10 mA/cm.² in 5 N-KOH (saturated with ZnO).
(*d*) Do. after 15 cycles, with ·1 gm./lit. of Lead Acetate.
(*e*) Micrograph of flake isolated after 13 cycles in 2·5 N-KOH (saturated with ZnO) + ·1 gm./lit. of Lead Acetate.

dissolution of zinc electrode or the working of a zinc accumulator are concerned, the only requirements are that the electrode remains active and reversible without the danger of undue powder formation or treeing and our work shows that this can easily be achieved by the addition of traces of lead ion.

References

1. Thirsk and Wynne-Jones .. *Trans. Inst. Met. Finishing*, 1953, **29**, Advance Copy 9.
2. Tope .. *Rev. Am. Electroplaters Soc.*, 1944, **31**, 229.
3. Eckardt .. *Korr. U. Metalls-hutz*, 1945, **21**, 14.
4. Huber, K. .. *Z. electrochem.*, 1942, **48**, 26.
   Helv. Chim. Acta, 1943, **26**, 1037; *Ibid.*, 1944, **27**, 1443.
5. Simmond and Ruder .. *J. Electrochem. Soc.*, 1951, **98**, 301.
6. Vahramain .. *Acta Physicochem.* (*URSS*), 1944, **19**, 148.
7. Morgan and Ralston .. *J. Electrochem. Soc.*, 1916, **30**, 229.
8. Hull and Wernlund .. *Trans. Electrochem. Soc.*, 1941, **80**, 407.
9. Titov and Paleolog .. *Khimi. Referat. Zhur.*, 1941, **4**, 84.
10. Lyons .. *J. Electrochem. Soc.*, 1954, **101**, 363; *Ibid.*, 1954, **101**, 376.
11. Dirkse .. *Ibid.*, 1954, **101**, 328.

947–57. Printed at The Bangalore Press, Bangalore City, by C. Vasudeva Rao, Superintendent and Published by The Indian Academy of Sciences, Bangalore.

NOTICE TO AUTHORS

Scientific papers intended for publication in the *Proceedings of the Indian Academy of Sciences* can be accepted only when they are communicated by a Fellow of the Academy whose duty shall be to satisfy himself that such communications are fit to be read at the Meeting of the Academy and published in its *Proceedings*.

Papers should not ordinarily exceed fifty pages of foolscap. MSS. should be either typewritten or written in legible hand on one side of the paper. All papers should be carefully revised by the authors and should be absolutely in final form for printing. Position for text-figures should be indicated. Each paper shall conclude with a critical summary not exceeding 350 words.

Drawings, diagrams or other illustrations should be made on larger scale (preferably) twice the size than the ones in which they are intended to appear. They should be done in Indian ink on bristol board with lettering in pencil. Scale of magnification of camera lucida tracings should be indicated by the side of drawings. In certain special cases arrangements will also be made for monochrome lithographic and other colour plates. Reduction of illustrations desired should be indicated in pencil. Appropriate legends should accompany all drawings. Names of authors are to be marked in pencil on the left-hand corner of drawing sheets. Photomicrographs should be securely mounted with colourless paste.

All tables, quotations and footnotes which will be set hereafter (beginning from Vol. I, No. 2) in types smaller than the text, should be typewritten on separate sheets and placed with the text in proper sequence. Footnotes should be numbered in Arabic numerals.

References to literature in the text should be given, whenever possible, in chronological order, only the names of authors and years of publication, in brackets, being given. They should be cited in full after the summary, the authors' names following in alphabetical order. Thus,

Name or Names of author; Name of Journal (abbreviation) with a single underline; Year of publication; Number of Volume with a double underline, and lastly page. The following would be a useful illustration:—

Bergmann and Stather . . . . . Z. Physiol. Chem., 1926, 152, 189.

Two copies of slip-proof and wherever possible, a page proof for final revision will be sent to authors. All corrections are best made on the slip-proof which should be transmitted to the Office of the Academy. All proof corrections involve heavy expenses which would be negligible if the papers are carefully revised by the authors before submission.

Fifty free reprints including plates and with cover will be supplied for each paper. Additional copies can be supplied at cost on previous intimation.

Blocks appearing in the *Proceedings* will be available for purchase by their respective authors. Orders for the same should be sent along with the corrected proofs and in any case not later than one month after the date of publication of the paper. The price charged would be 25% of the actual cost of the blocks *plus* freight and despatching charges. If the blocks are reproduced in other journals or publications, due acknowledgment should be made in them to the *Proceedings*.

The original drawings and plates of blocks appearing in the *Proceedings* will be returned to such of the authors as may require them provided the cost of despatching such originals is borne by them.

CONTENTS

PAGE

Emission Spectrum of Bromine Excited in the Presence of Argon—Part I . . . . . Putcha Venkateswarlu and R. D. Verma 251

Synthetic Experiments in the Benzopyrone Series. Part LXVI. Relative Stability of Isomeric 6-Methyl and 8-Methyl-Trihydroxy Flavones . . . . V. V. S. Murti, T. R. Seshadri, V. Sundaresan and B. Venkataramani 265

The Localisation of the Discharge Channel in a Glow Discharge . . . . . V. T. Chiplonkar, J. Mangaly and Kumari D. V. Nagamani 272

Heterocyclic Compounds. Part X. Synthesis of 14, 15, 16, 17-Tetrahydro-16-Keto-17-Aza Cyclopenta-(*a*)-Phenanthrene and Substituted 1-Cyclopenta-(*c*)-Quinolines . . . . . S. Kanthamani 277

Light Propagation in Absorbing Crystals Possessing Optical Activity . . . . . S. Pancharatnam 286

The Rate of Hydrolysis of Chloroacetamide in Aqueous Acid . . . . . Sundaresa Soundararajan and Marjorie J. Vold 293

Electro-Deposition and Dissolution of Zinc in Zincate Solutions . . . . . Indra Sanghi and W. F. K. Wynne-Jones 305